

LASER INTERFEROMETER GRAVITATIONAL WAVE OBSERVATORY  
-LIGO-  
CALIFORNIA INSTITUTE OF TECHNOLOGY  
MASSACHUSETTS INSTITUTE OF TECHNOLOGY

<b>Technical Note</b> x/xx/99	<b>LIGO-T9900xx- 00- D</b>
<b>Fumiko Kawazoe</b>	
Author(s)	

This is an internal working note  
of the LIGO Project.

**California Institute of Technology**  
**LIGO Project – MS 51-33**  
**Pasadena CA 91125**  
Phone (626) 395-2129  
Fax (626) 304-9834  
E-mail: [info@ligo.caltech.edu](mailto:info@ligo.caltech.edu)

**Massachusetts Institute of Technology**  
**LIGO Project – MS 20B-145**  
**Cambridge, MA 01239**  
Phone (617) 253-4824  
Fax (617) 253-7014  
E-mail: [info@ligo.mit.edu](mailto:info@ligo.mit.edu)

WWW: <http://www.ligo.caltech.edu>

## **ABSTRACT**

LIGO's 40 meter interferometer is now testing a RSE scheme for Advanced LIGO. In order for the interferometer to work properly one of the most important things is to maintain the optics position and orientation.

OSEM system controls the position of the optics and Oplev system is used to monitor the angular orientation of the optics.

My work includes resetting up the system, calibrating its response, characterizing noise in the system and closing the control loop as I participate in the 40 meter project from the summer of 2003 to the summer of 2004.

# 1 Introduction

## 1.1 Gravitational wave

Gravitational waves are ripples in space-time produced by accelerating masses such as celestial objects. Einstein predicted the existence of gravitational waves in 1916 in his General theory of relativity. As a consequence of Einstein's equation under the approximation that space-time is nearly flat disturbance of the curvature of space-time propagates at the speed of light. The perturbation of flat space-time is represented by  $h_{\mu\nu}$ . As a wave passes it changes the space-time interval, stretching it in one direction (x-axis) and compressing it in the other (y-axis). Figure 1 visualizes the gravitational wave effect on a set of free-falling test masses. The wave described in Figure 1 propagates vertically through the paper (z-axis) and the polarization states are orthogonal to the direction of the propagation (x-y plane). These states are called plus and cross ~~more~~ and their polarization axes are  $\pi/4$  rotated from those of each other as shown in Figure 1.

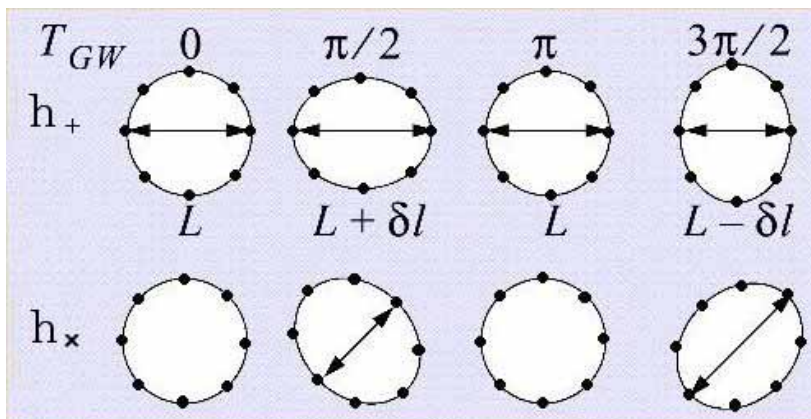


Figure 1: Two polarization states of a gravitational wave ~~which is~~ passing through the plane of the paper. It shows how the wave stretches and compresses the distance between test masses.

The ratio of the distance between test masses to the deviation caused by a wave is expressed in strain  $h$ . The strain is so small, making the direct detection of gravitational waves so challenging. For example waves emitted

by a binary neutron star pair each of whose mass is 1.4 solar masses, located about 15 Mega pc away would emit a gravitational wave whose strain is  $h \approx 1 \times 10^{-21}$ .

## 1.2 Principle of detection

To directly detect the strain caused by gravitational waves Michelson interferometer will make a proper device since it can measure the difference in length of the two arms. As shown in Figure 2 when a wave passes through the Michelson interferometer it stretches one arm and shrinks the other. The interferometer is set in such a way that when it is free from gravitational waves the output port is kept dark (dark port). The length change can be detected from the power in dark port. Because the strain is a ratio between the displacement a wave causes ( $\Delta L$ ) and the interferometer arm length ( $L$ ) with a larger  $L$  the detector's sensitivity to the signal can be increased.

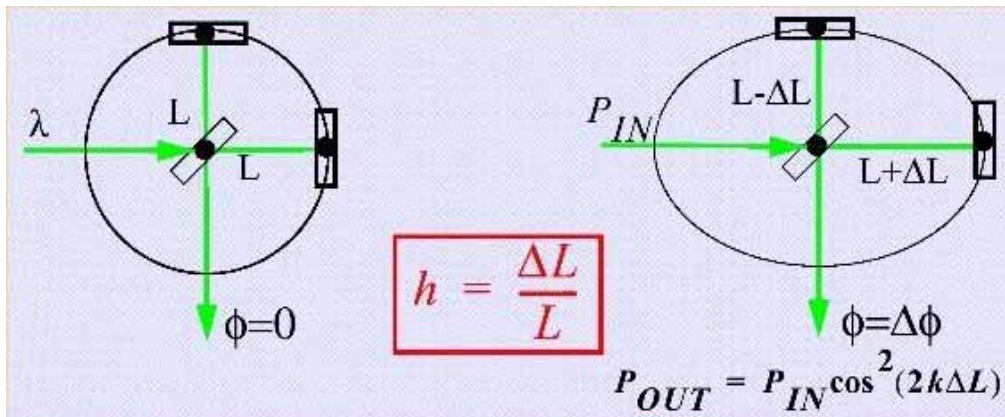


Figure 2: A Michelson interferometer as a gravitational wave detector.

## 1.3 World project

There are several large interferometers in the world such as LIGO, VIRGO, GEO and TAMA. These are the first generation detectors some of which started operating. The second generation detectors are also planned to be operated in the near future and among them are Advanced LIGO and LCGT.







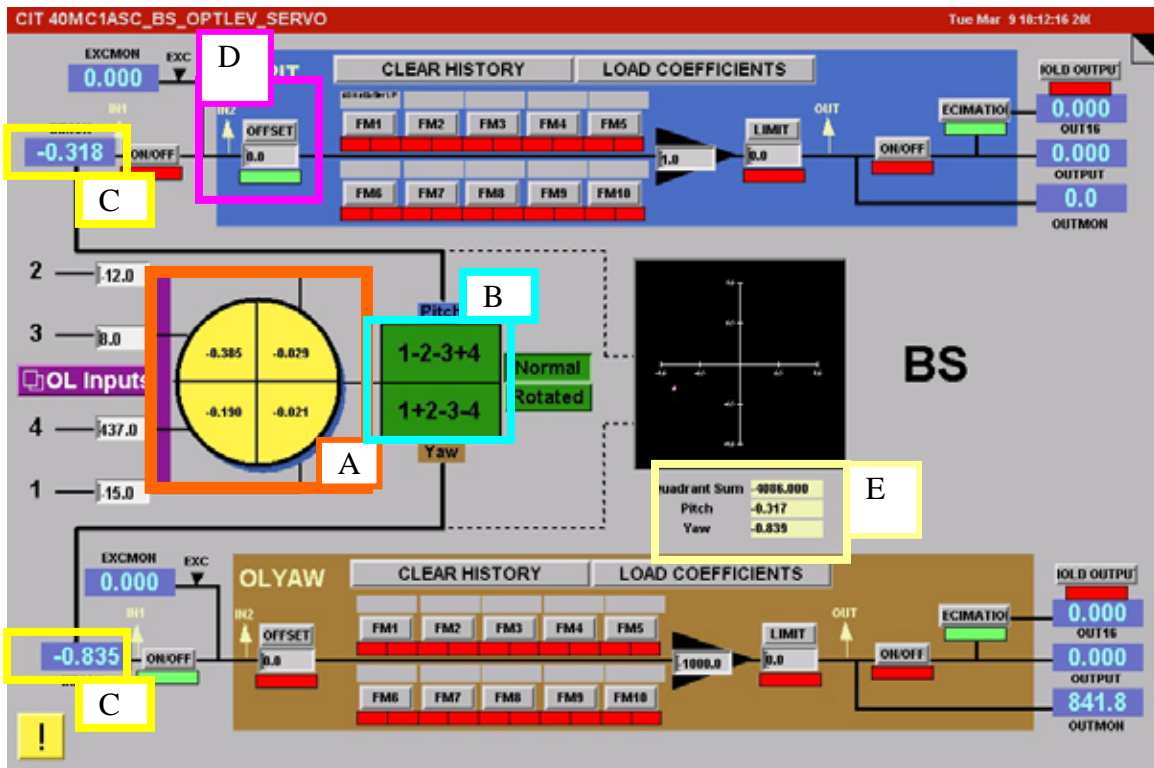


Figure 4: The EPICS screen reading out the signal

### 2.2.1 The measurement principle

In order to calibrate the displacement signal to the angular motion of the optic, the signals are read from the EPICS display when a known small position displacement is added to the beam path then the angle displacement of the optics that would give the same position displacement to the beam will be calculated.

To give a known small position displacement, a prism is a proper device because it gives a small shift to the exit beam due to the light refraction effect. Snell's law describes how much shift the prism adds to the incident beam and when the wave length of the beam, the incident angle and the index of refraction of the air and the prism are known the shift can be calculated. The calculation of the beam shift and the angular displacement are shown in the Figure 5 and 6 respectively in Appendix 2.

## 2.2.2 Calibrating method

The measurement for all 5 optics was done in the way described below.

### Yaw measurement

1: The offset of the Oplev input was adjusted so that when there is no light on the QPD the output monitor (c1:sus-suspension name\_OL1~4\_OUTMON) oscillates around 0. (See Figure 7). The output monitor port (c1:sus-suspension name\_OL1~4\_OUTMON) shows values about 6500 times larger than the actual output (c1:sus-suspension name\_OL1~4\_OUTPUT) so that it is more useful to read this value when there is little light on the QPDs as shown in Figure 8.

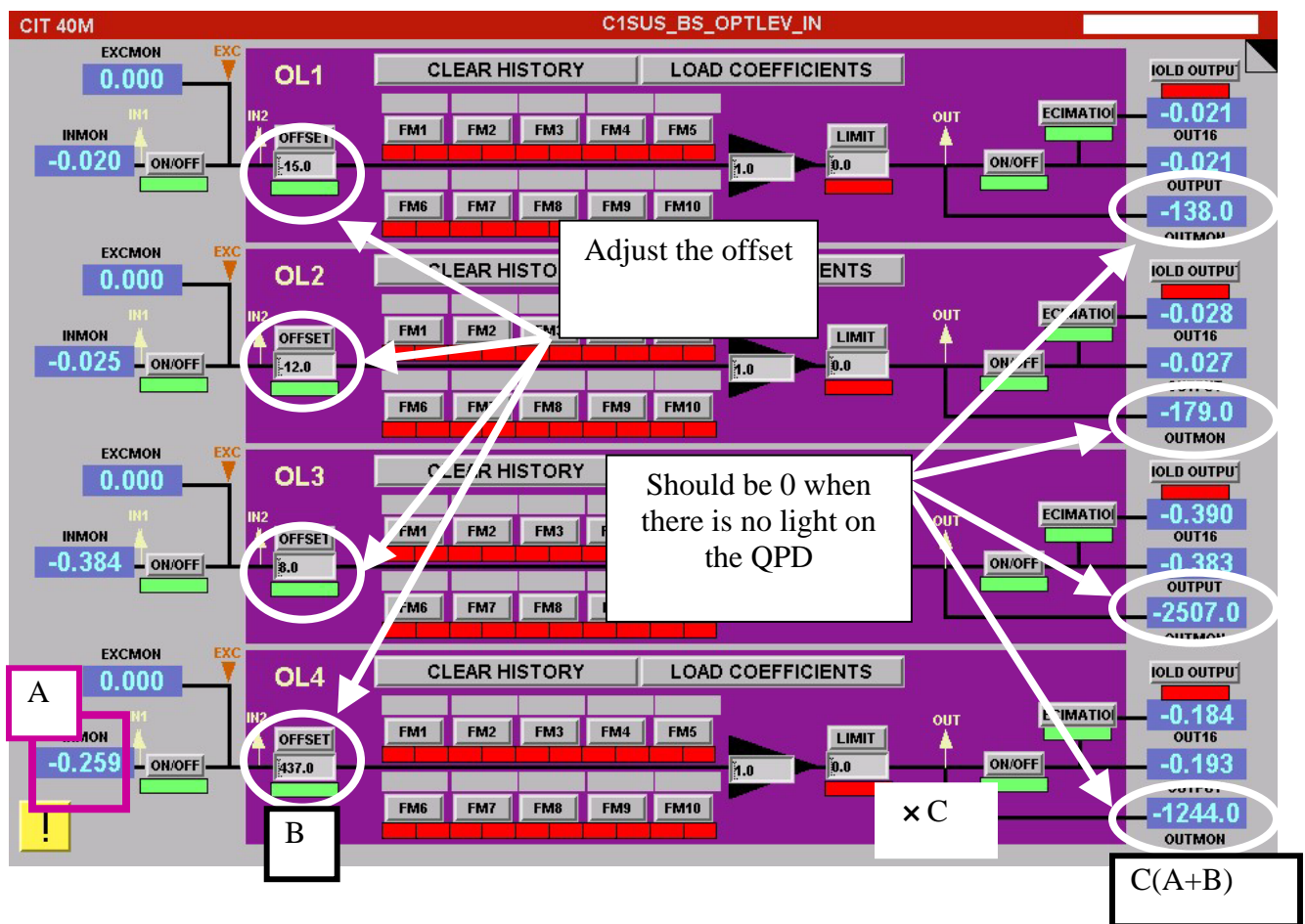


Figure 7: The offset (B) is adjusted and added to the input (A)  
 So that when there is no light hitting the QPD the output of the QPD is 0.

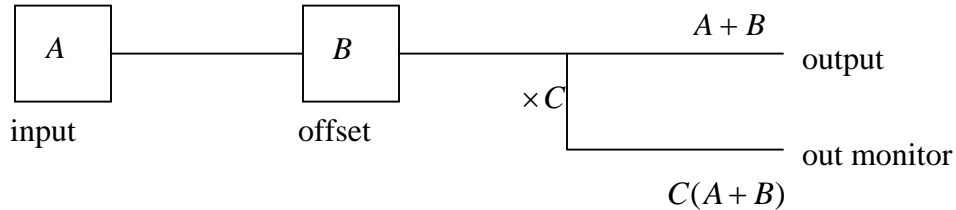


Figure 8: A diagram which shows the signal flow from the input to the output. Here C is about 6500 and it is useful to use the out monitor port when there is little light on the QPD.

2 : The beam was centered on the QPD.

3: The prism on a rotary mount was placed in front of the QPD as shown in Figure 9. The distance between them is approximately 10cm. Since the prism is slightly wedged it was made sure the wedge is in vertical direction so that the initial beam is horizontally parallel to the outgoing beam as shown in Appendix 3.

4: Placing the prism in front of the QPD may change the beam height a little. First the beam on the prism was centered and it was made sure that the beam was horizontally centered on the QPD. Then the beam height was readjusted so that it hits the center of the QPD.

5: The yaw value was read from the output port (C1:SUS-suspension name\_OL\_yaw) as the B part of the prism in Figure 9 was rotated every 2 degrees in both positive and negative angle until the signal gets saturated.

6: Plot the data

The data were plotted and only that of the linear region were selected to fit to a linear function ( $y = a \times x$ ). By fitting the data to the function the calibration factor was obtained.

## Pith measurement

1: The same thing was done except in doing 3 it was made sure that the wedge is in horizontal direction so that the incident beam is vertically parallel to the exit beam.

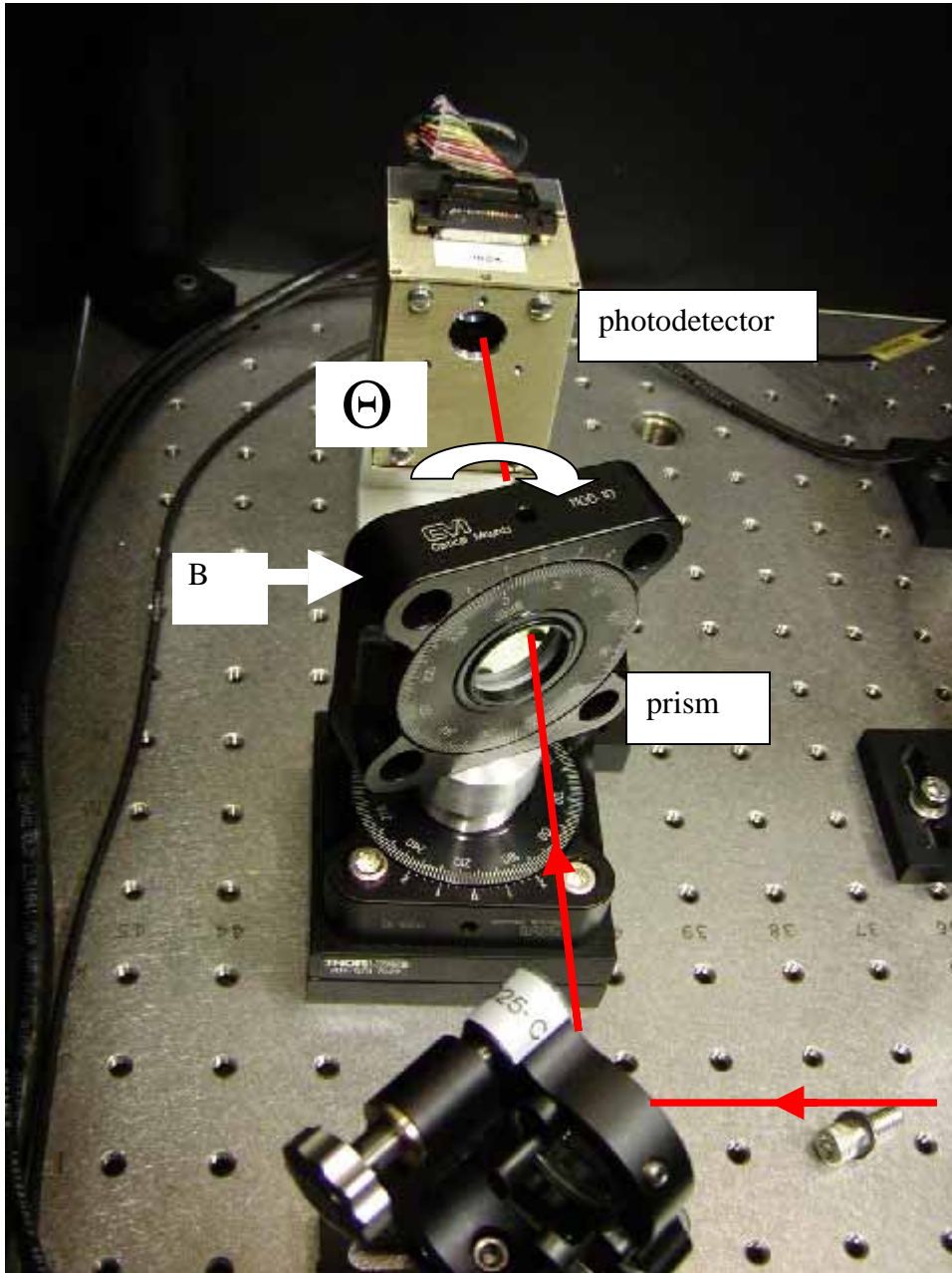


Figure 9: The setup of the Yaw measurement.

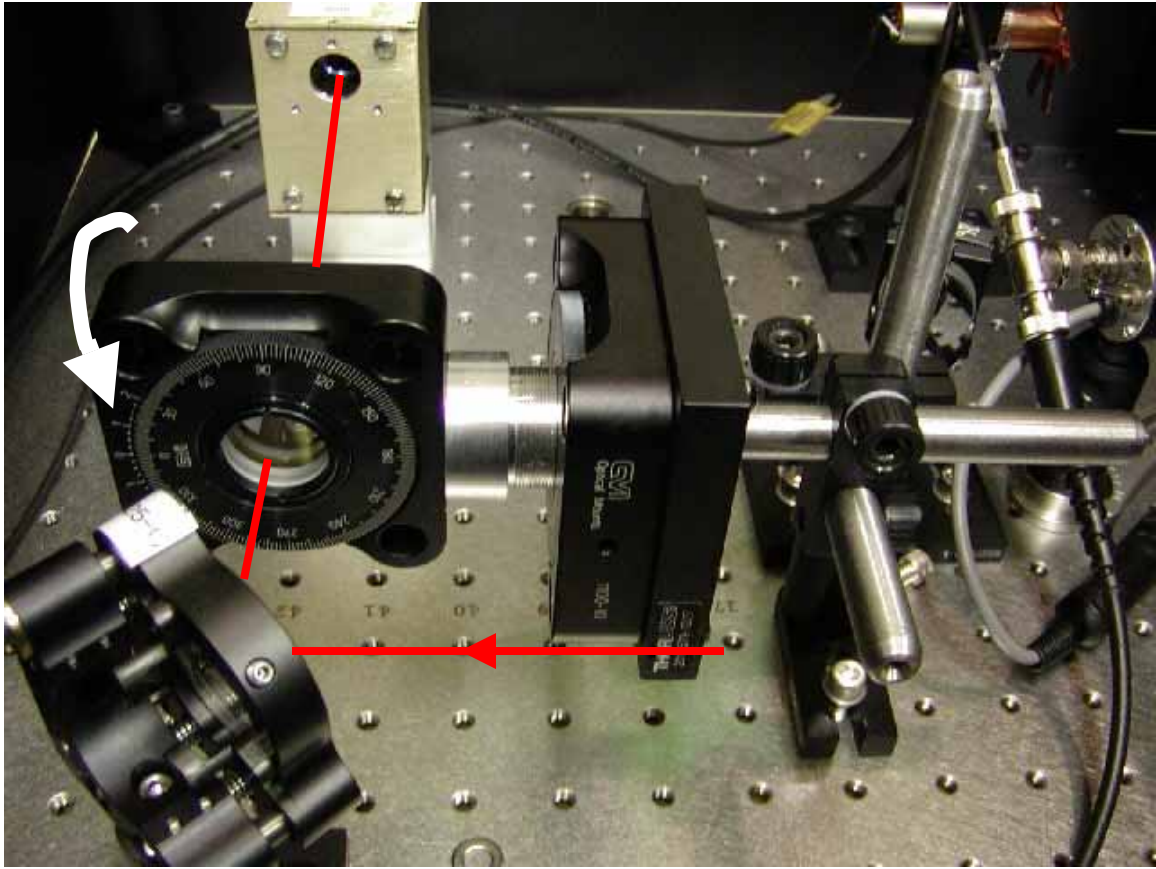


Figure 10: The setup of the Pitch measurement

### 2.2.3 The result

The calculated calibration factors are listed below.

Optics	Pitch calibration factor	Yaw calibration factor
ITMX	8333.21	7271.8
ITMY	6047.06	6874.36
ETMX	5968.07	5713.55
ETMY	5975.98	5940.79
BS	6737.3	8263.33

Chart 2: The calculated calibration factors of the 5 optics.

The plots that show the results are shown in the Appendix 4.

### 3 Oplev system sensitivity

To have the Oplev signals feedback on the optics to damp their motion it is essential to verify the frequency region where the sensitivity of the Oplev system is well enough that the feedback can be properly applied to the system. In order to verify that the Oplev signals contain the information of the optics angular motion noise characterization was done.

#### 3.1 Expected noise sources in the system

There are several possible noise sources in the Oplev system. Noises appear in the output of the system which will be feedback to control the optics.

There are three main expected noise sources in the system; a seismic noise, a beam jitter noise and an electronic noise.

The Oplev system is on the optical tables which don't have seismic attenuation systems, the seismic noise in the Oplev systems are expected to be larger than that of the table on which the optics are placed.

The beam jitter noise from the 670nm lasers is expected to be relatively large due to the quality of the lasers.

The electronic noise comes into the system from various places and is expected to be in the higher frequencies.

As attempts to measure each of these noises were made, it turned out that the beam jitter noise and the seismic noise are almost impossible to separate from the signal at the moment due to too many uncertainties in the measurements: (e.g. the optical table for BS Oplev is on the additional plate which is placed on the floor, making the table shake differently than other tables, but BS optical table is the one which is able to be used for the measurement.)

#### 3.2 Noise characterization

Although it is impossible to measure each of the noise sources at the moment, it is possible to measure the total noise and search the frequency region where it is dominated by the noise due to the angular motion of the optics.

When it is assumed that the optical tables follow the seismic movement at lower frequencies, the RMS noise of the tables can be expressed as the typical RMS spectrum of seismic noise which can be approximated to

$$S = \frac{10^{-7}}{f^2} [m/\sqrt{Hz}]$$

The RMS noise of the optics motion caused by the ground motion can be approximated by applying transfer functions of the tree stacks and the transfer function of the pendulum to the spectrum of the seismic noise. The tree stacks' transfer functions and the damped pendulum transfer function can be written as

$$H = Abs \left[ \frac{\omega_i^2 + j \frac{\omega_i \omega}{Q_i}}{\omega_i^2 + j \frac{\omega_i \omega}{Q_i} - \omega^2} \right] \text{ here, the subscript } (i = s1, s2, s3, p) \text{ is used to}$$

represent the three stacks (stack 1, 2 and 3) and the pendulum respectively. Their Q factors and resonant frequencies are listed below in chart 3.

	Resonant frequency	Typical Q-factor
Pendulum yaw	0.5	10
Stack1	8.5	4.2
Stack2	22	4
Stack3	40	4

Chart 3: The resonant frequencies and the typical Q-factors of the pendulum and the three stacks.

The typical seismic spectrum and the optics motion spectrum are plotted in Figure 19.

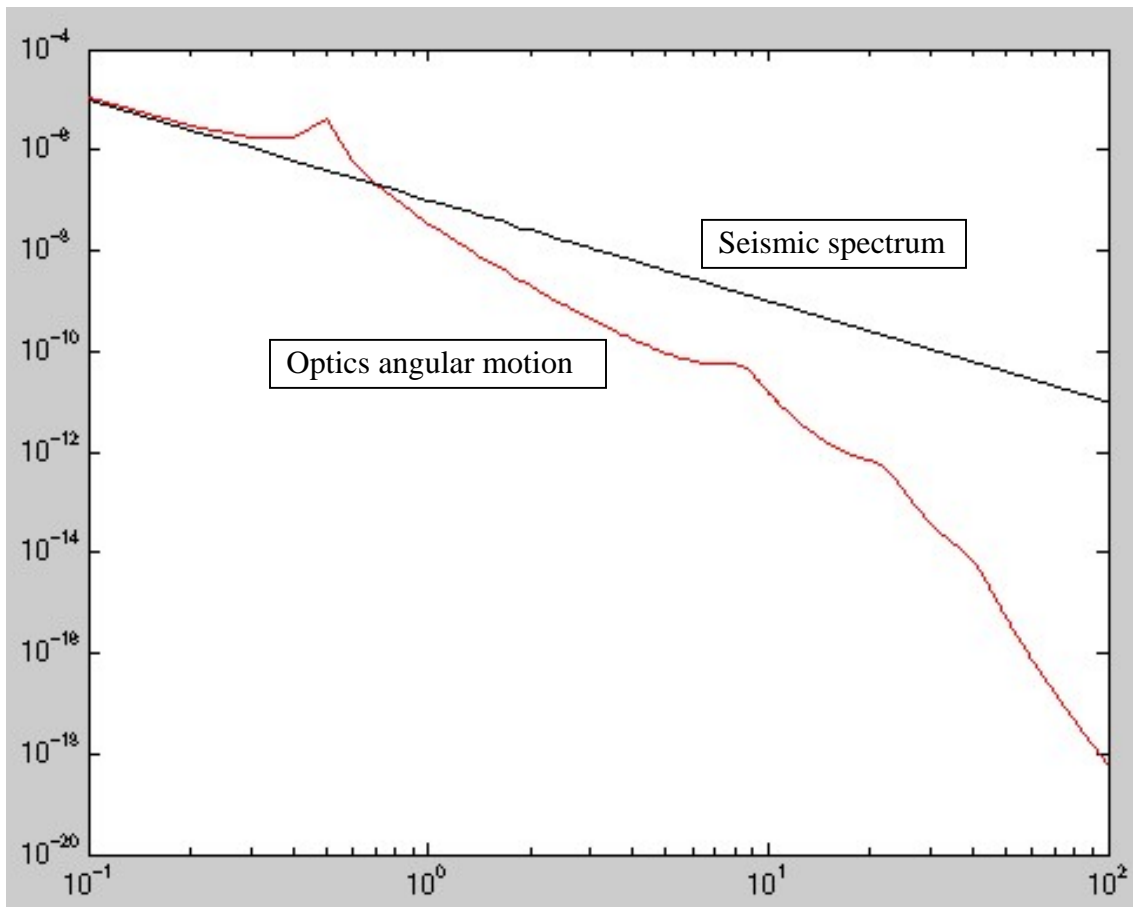


Figure 19: The spectra of the optics angular motion and the seismic noise.

From Figure you can see that around optics' resonant frequencies the noise from the optics can be detected which can then be feedback to control the optics.

The noise was also measured to verify that the noise from the optics' angular motion dominates the total noise at the resonant frequency. The noise was measured with two settings; one with the beam hitting the optic and the other without the beam hitting the optic. Comparing these should tell if the noise due to the optic's motion dominates at its resonant frequency. Figure 20 shows the two settings. Here ETMY was selected because it has enough space on the optical table for the measurement.

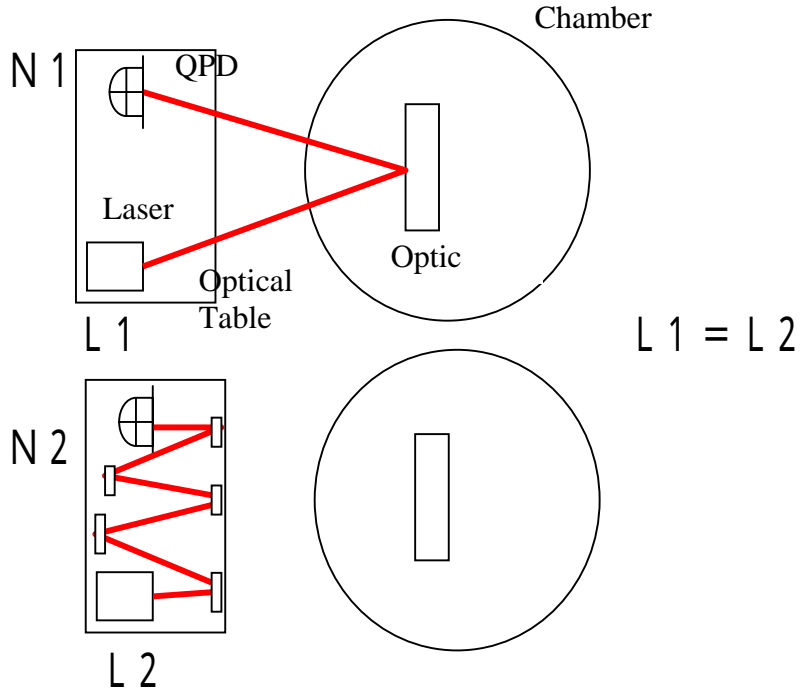


Figure 20: The set up of the noise measurement; one with the beam hitting the optic and the other not hitting it.

The noise spectra of yaw and pitch were taken from C1:SUS-ETMY\_OLPIT/YAW\_IN1. The beam path are all the same (347.2cm). The spectra is shown in Figure 21 below.

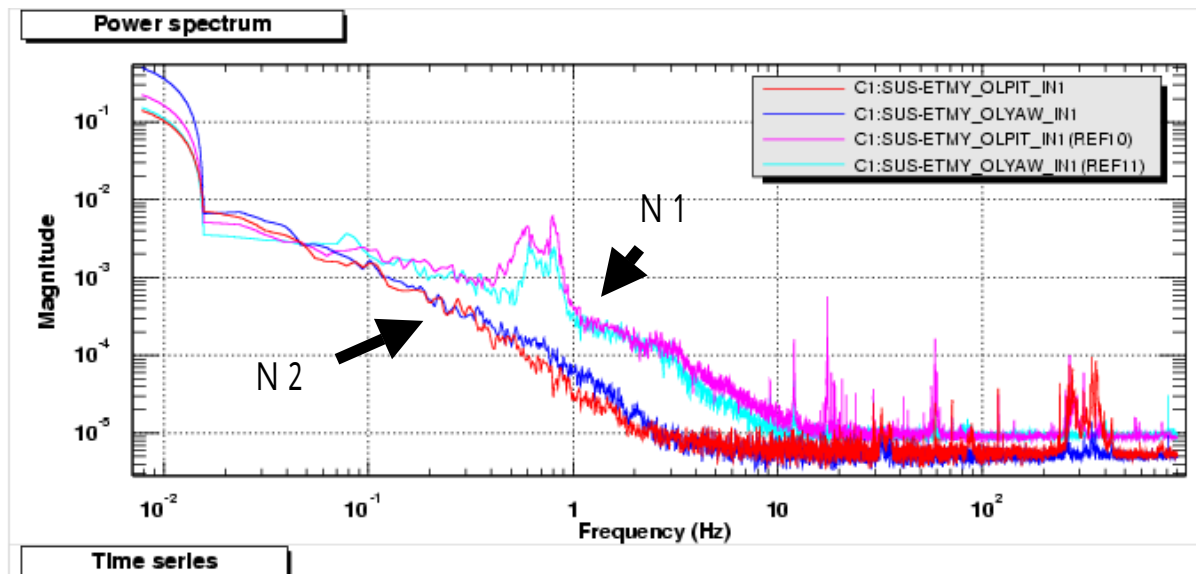


Figure 21: The noise power spectra of pitch and yaw.

N1 includes the noise from the optic while N2 doesn't. From the figure can be concluded that around the resonant frequency the optics motion dominates the total noise.

This result indicates that the optics can be controlled with proper feedback loop at around the vicinities of the resonant frequency.

#### 4.1 Controlling the optics

In order to control the optics to damp their motion at around their resonant frequencies the Oplev signals have to be feedback on the optics through the control loop. Figure 22 shows the control loop of the system. It is a negative feedback loop.  $V_{in}$  is the reference and  $V_{out}$  is the sensor signal. The goal is to make  $V_{out}$  small.

Without closing the feedback loop the noise introduced to the suspended optics will be amplified by the suspension resulting in a large motion of the optics at the resonant frequency.

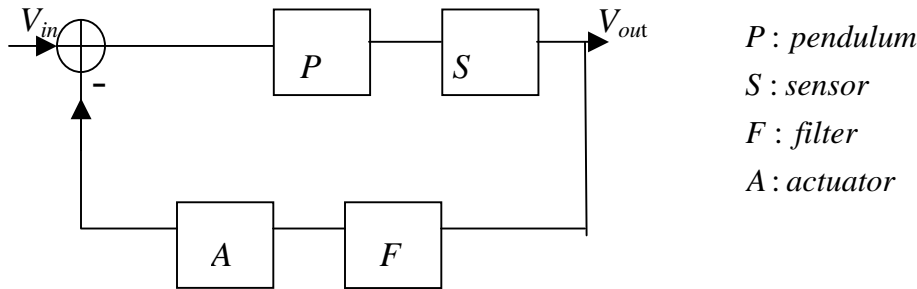


Figure 22: Oplev control loop.

When the loop is closed as shown in Figure 22,  $V_{out}$  can be expressed as  $V_{out} = \frac{PS}{1+G} V_{in}$  where the open loop gain  $G = PSFA$ . When

$G \gg 1$  this becomes

$V_{out} = \frac{PS}{G} V_{in} = \frac{1}{FA} V_{in}$ . By designing a proper filter  $F$ ,  $V_{out}$  can be

optimized and the Q-factor can be changed. Figure 23 explains how the Q-factor is changed. Where the open loop gain  $G$  is much larger than 1 the sensor signal will be reduced inversely proportional to the gain at the same frequency region making  $Q \approx \frac{Q_0}{G}$ . The filter here is a high-pass filter with a zero at 0Hz and two poles at 3 Hz.

Measuring the Q-factor of the system will tell how well the optic is damped.

The ideal case is when the optic is critically damped although trying to achieve critical damping by OSEM system is noted to cause noise at higher frequencies and this limits how much the OSEM can damp the optics. Thus it is important to use Oplev system to help damp the optics. In order to see how much Oplev system together with the OSEM with its typical value of gain can damp the optics, the Q-factor was measured with various values of the Oplev filter gain with a fixed OSEM gain which is typically used.

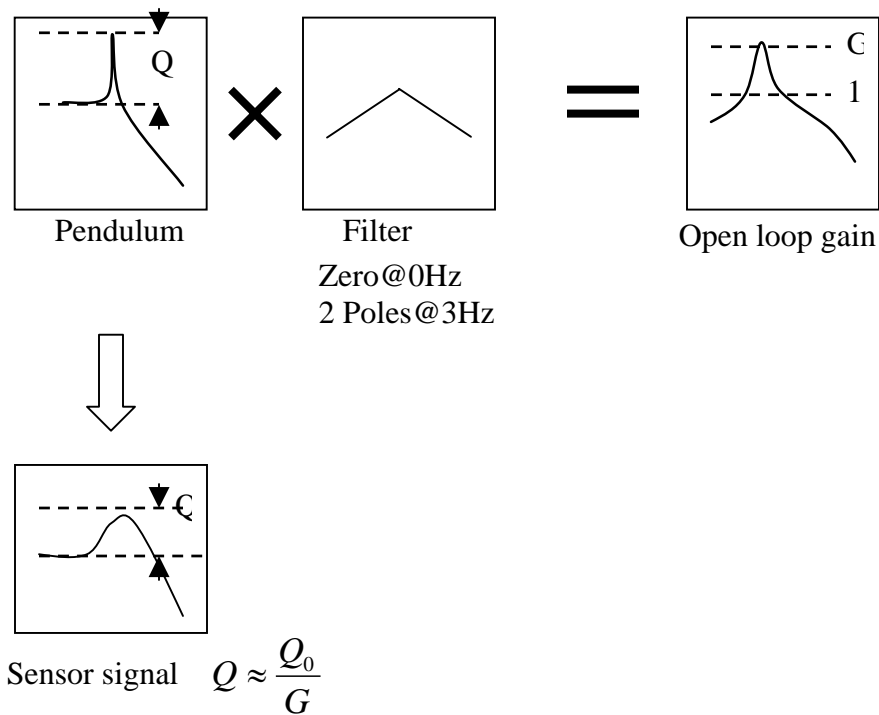


Figure 23: How the Q-factor can be changed by closing the control loop.

To observe the Oplev system damp the optics, the transfer function of the suspended optics are measured and the Q-factors were calculated using the software LISO.

As a result we observed the Oplev damp the optics close to critical damping which is represented as a dashed blue line as shown in Figure 24 and concluded that with a proper modification to the filters the Oplev system can be used to help damp the optics motion at the resonant frequency. From Figure 24 it seems that the value of the Q-factor decreases as the inverse square root of the value of the gain instead of as the inverse of the value of the gain. This is because the damping is caused not only by the Oplev system but also by the OSEM system, and when the gain of these two systems are comparable the rate of contribution of the Oplev gain to the system will be decreased and the slope will be gentler.

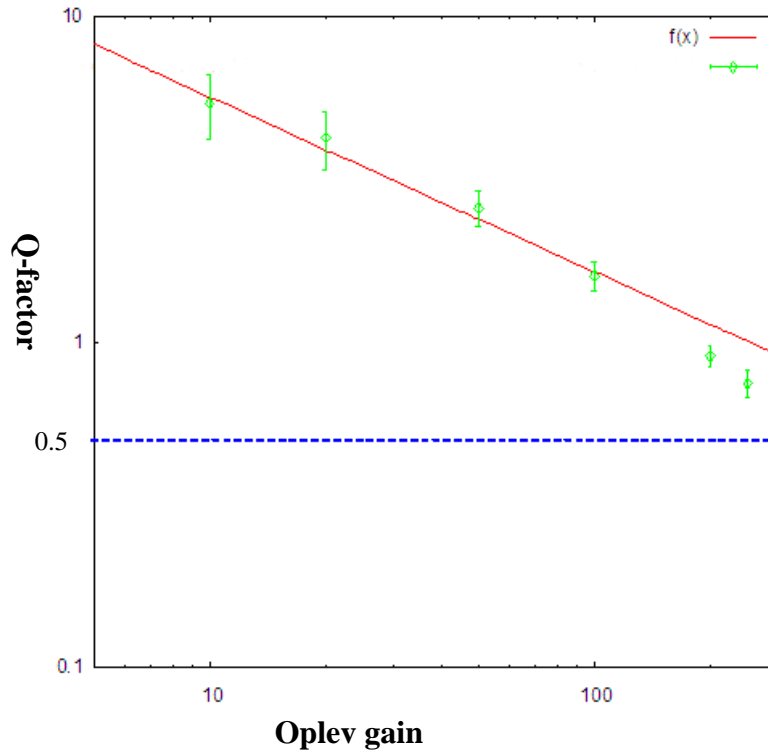


Figure 24: The relationship between the Q-factor and the Oplev gain. When the system is critically damped the gain is 0.5 as represented by the dashed blue line.

## 4.2 Designing digital filters for Oplev control loop

In order to reduce the noise at the resonant frequencies and make it possible to help control the optics by Oplev system, digital filters for each of the seven optics was designed using the software Foton.

Each optic has the filters listed below in Chart 3. The high-pass filter has a zero at 0 Hz and two poles at 100 Hz. The resonant gains are placed at position resonant frequencies because there is strong couplings with position and pitch or yaw motion and motion at position resonant frequency tend to be larger.

		Zero (Hz)	Pole (Hz)	Resonant gain (Hz:Q:dB)
ITMX	Pitch	0	100,100	(0.8:5.3:40)
	Yaw	0	100,100	(0.8:5.3:30)
ITMY	Pitch	0	100,100	(0.8:4:14)
	Yaw	0	100,100	(0.8:2:10)
ETMX	Pitch	0	100,100	(0.8:3.2:20)
	Yaw	0	100,100	(0.8:5:20)
ETMY	Pitch	0	100,100	(0.8:8:26)
	Yaw	0	100,100	(0.8:4:20)
BS	Pitch	0	100,100	(1:10:30)
	Yaw	0	100,100	(1:10:30)
PRM	Pitch	0	100,100	
	Yaw	0	100,100	
SRM	Pitch	0	100,100	
	Yaw	0	100,100	

Chart 4: Oplev filters

(\*while this process of designing and implementing the filters it was discovered that although EPCS screen shows that the sampling rate of Oplev servo is 16384Hz, it actually is 2048 Hz, thus when making digital filters sampling rate of 2048 Hz should be selected on Foton.)

### 4.3 In-loop noise measurement

All the optics noises were measured from the port (C1: SUS-opticsname\_OLPIT/YAW\_IN1) when the feed back loop is on /off. It reads the suspension output signal. The gain of the filters are set in such a way that it gives enough damping performance but small enough that it does not cause the oscillation in the system. The gain of the OSEM control loop is optimally set previously.

## 4.4 Results

The results are shown in Appendix 5. We observed that with the control loop on all the optics are well damped.

## 5 Future work

With the control loop Oplev helps OSEM damp the optics properly at the region of resonant frequencies. As the noise characterization at higher frequency is getting realistic, the filters have to be modified properly to suppress noises in that region of the frequency. The gains have to be adjusted so that the combination of the OSEM and Oplev control loops can perform at their best.

## Appendix 1

Optics	Change made to the system
ITMX	Beam path shortened (203.6:270.2:473.8) Number of stirring mirror in the path (5)
ETMX	Beam hits the AR side of the optics Beam path shortened (133.6:167.5:301.1) Number of stirring mirror in the path (3)
ITMY	Beam path shortened (251.5:181,9:433.4) Number of stirring mirror in the path (6)
ETMY	Beam hits the AR side of the optics Beam path shortened (157.4:192.8:350.2) Number of stirring mirror in the path (3)
BS	Beam path shortened (251.1:363.9:615) Number of stirring mirror in the path (7)

Chart 1: Changes made to the existing Oplev system.

The beam path length is expressed in cm.

a and b of (a:b:c) represents the beam path length from the laser to the optic (incident beam), the length from the optic to the QPD (returning beam) and the total length respectively.

## Appendix 2

The beam shift ( $\Delta x$ ) is caused by the prism.  
According to Snell's law, the relationship between angles of incidence and refraction for the beam can be written as

$$\frac{n_1}{n_2} = \frac{\sin \theta_2}{\sin \theta_1}$$

From which the displacement  $\Delta x$  added to the incident beam can be calculated as below.

$$\frac{n_1}{n_2} = \frac{\sin \theta_2}{\sin \theta_1}$$

$$\rightarrow \sin \theta_2 = \frac{n_1}{n_2} \times \sin \theta_1$$

$$l \cos \theta_2 = d$$

$$\rightarrow l = \frac{d}{\cos \theta_2}$$

$$\Delta x = l \sin(\theta_1 - \theta_2)$$

where

$\theta_1 \dots$  angle of incidence

$n_2 \dots$  index of refraction of air = 1.0003

$\theta_2 \dots$  angle of refraction

$n_1 \dots$  index of refraction of the prism (BK7)

for 670nm wave length = 1.51391

$d \dots$  prism thickness = 6.35mm

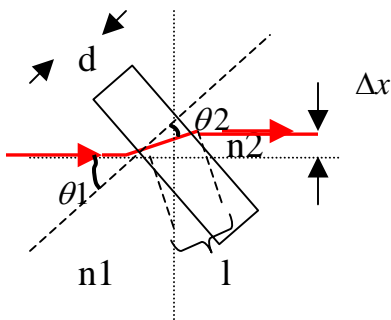
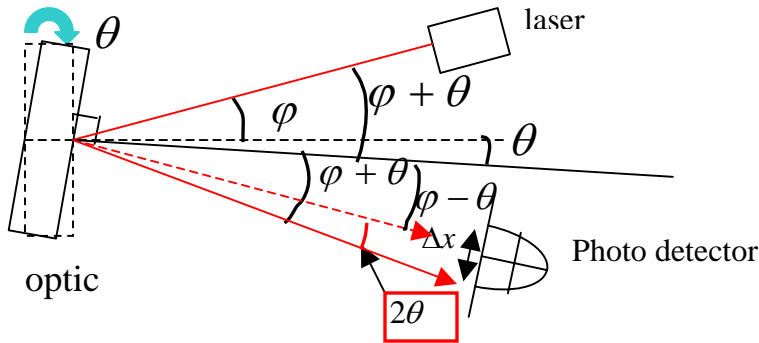


Figure 11: The beam shift caused by the prism.

Angular displacement is calculated in the way described below.

The laser is incident on the optic. The position displacement on the photo detector  $\Delta x$  is given the angular displacement of the optic that would give the displacement can be calculated as written in Figure 6.



where

$$R \times 2\theta = \Delta x$$

$$\rightarrow \theta = \frac{\Delta x}{2R}$$

$\phi$ ..... angle of incidence

$\Delta x$ ... position displacement

$R$ ..... return beam path length

$\theta$ ..... angular displacement of the optic

Figure 12: The calculation of the angular displacement of the optic.

## Appendix 3

### The correction of the wedge effect

Because the prism is slightly wedged, the wedge should be in vertical direction so that the initial beam and the exit beam are horizontally parallel.

To make sure the wedge is in vertical direction, the reflected beam from the prism was monitored as the part A in Figure 10 was rotated. As it rotates, the reflected light also rotates and the trace was monitored on a material which refracts the beam (e.g. a piece of paper). When the reflected beam is at the top and the bottom of the circle, the wedge is in vertical direction. (See Figure 10) The reason why the reflected beam was used is that it was more convenient to monitor the reflected beam because of the limited space on the Oplev table.

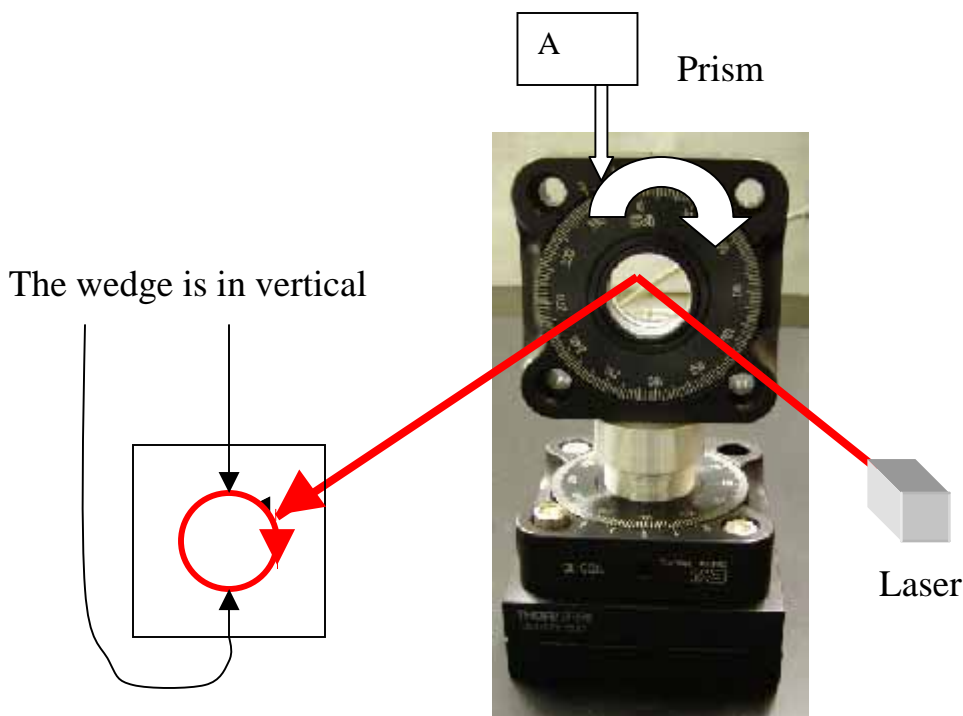


Figure 13: The way to find when the

## Appendix 4: The Oplev response to angular displacement

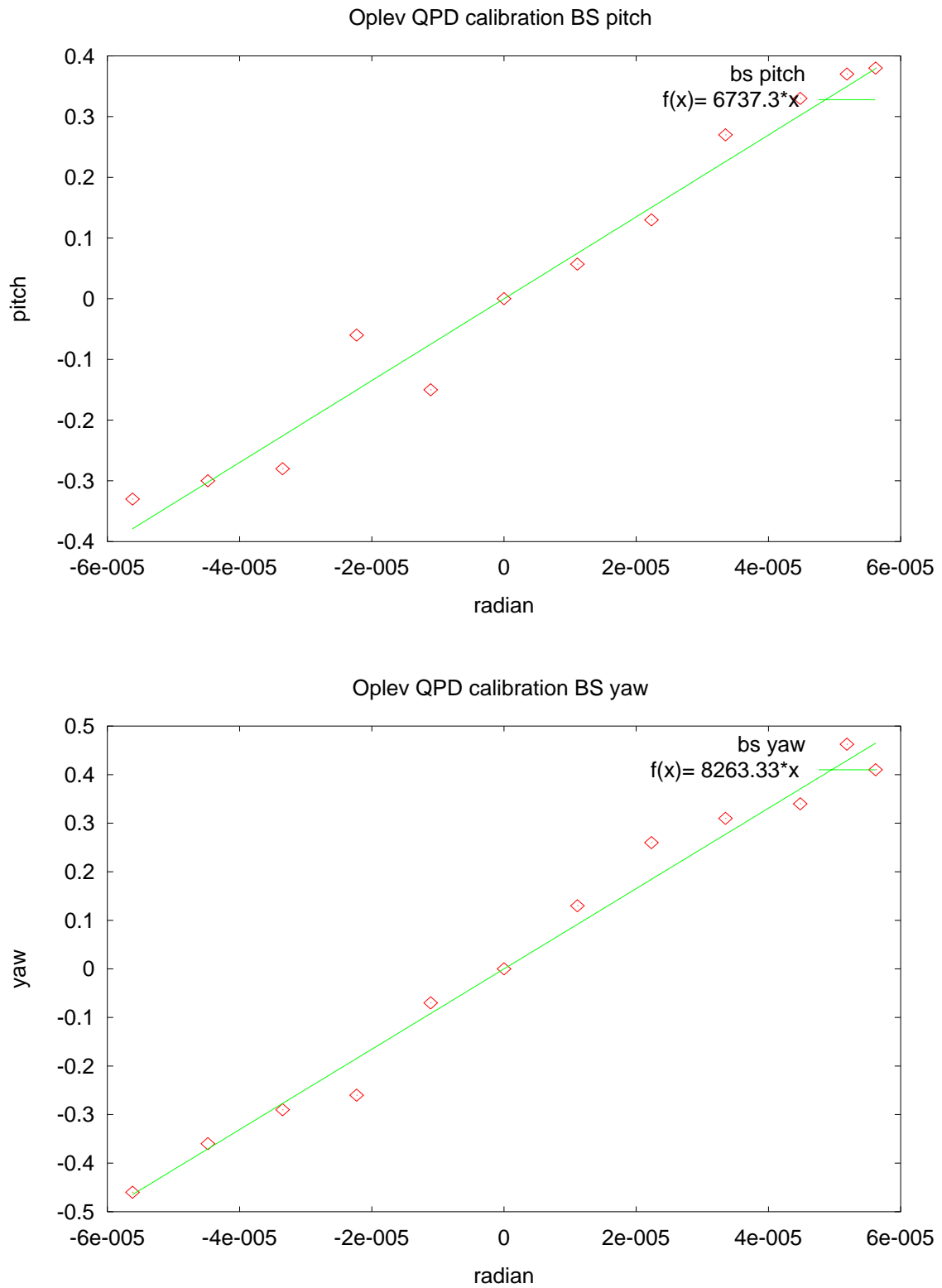


Figure 14: BS pitch and yaw

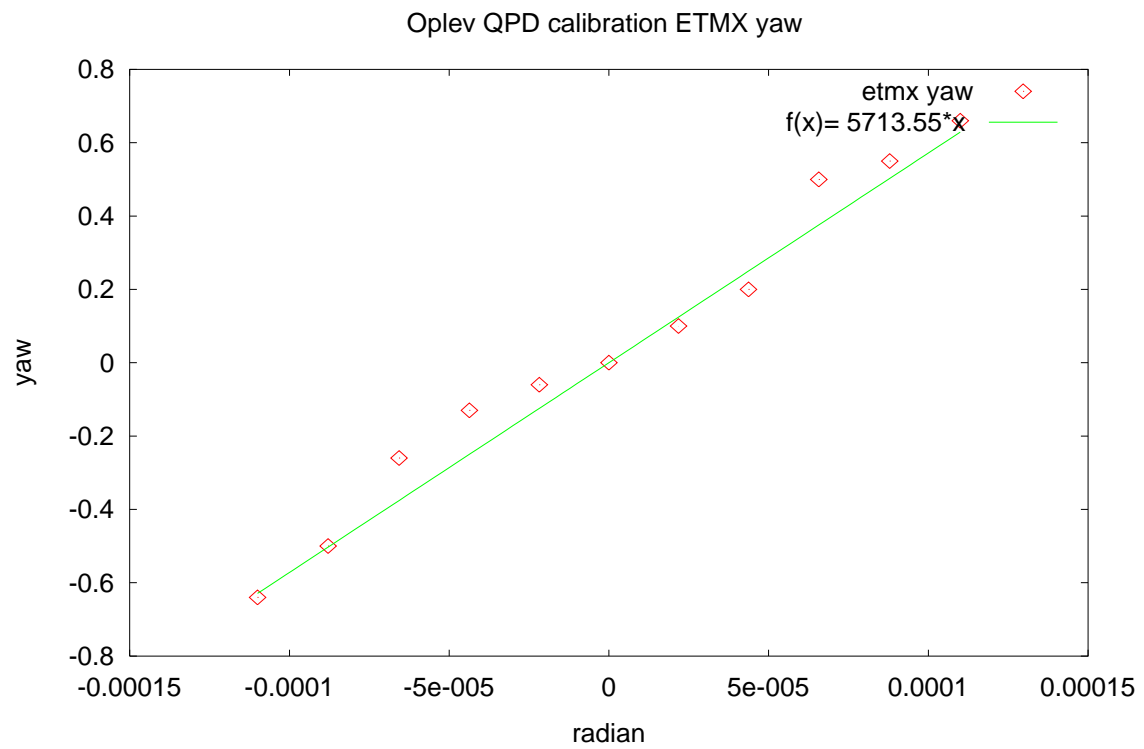
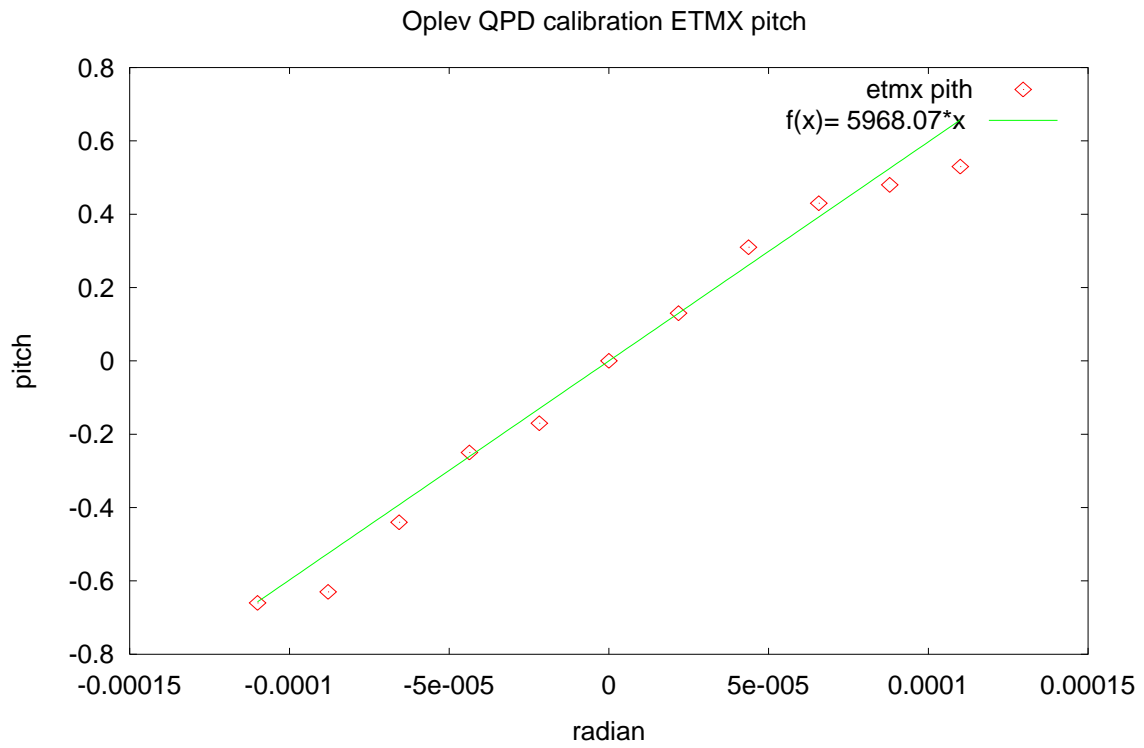


Figure 15: TEMX pitch and yaw

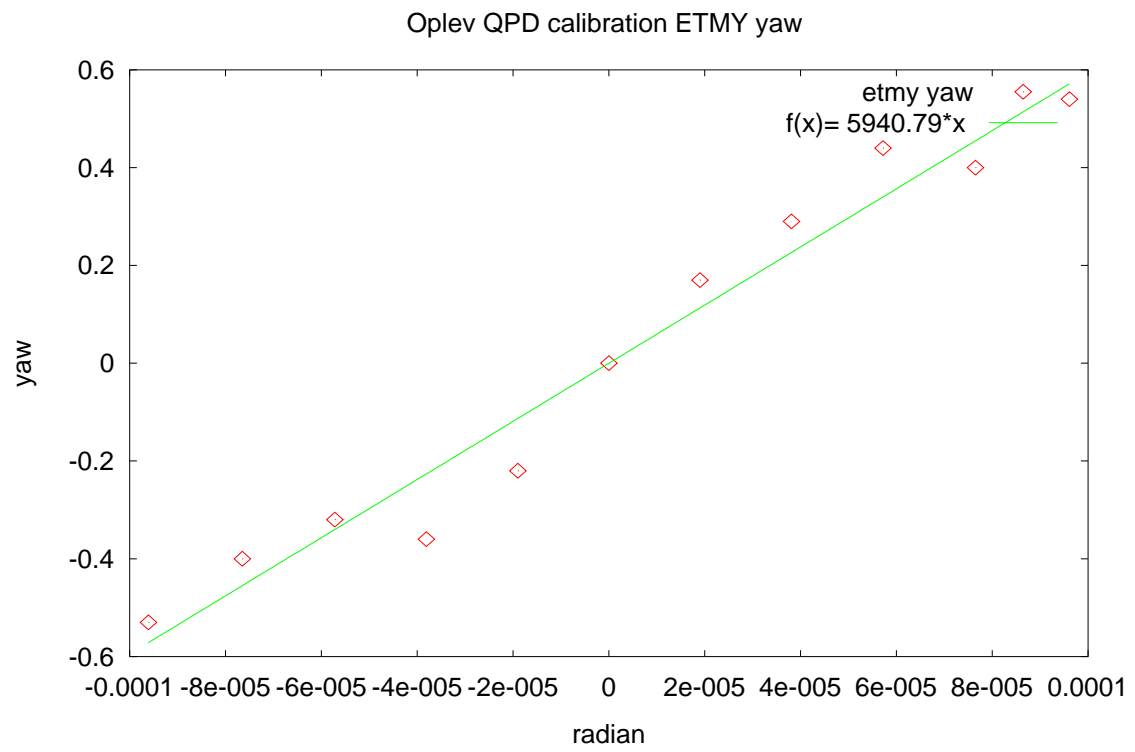
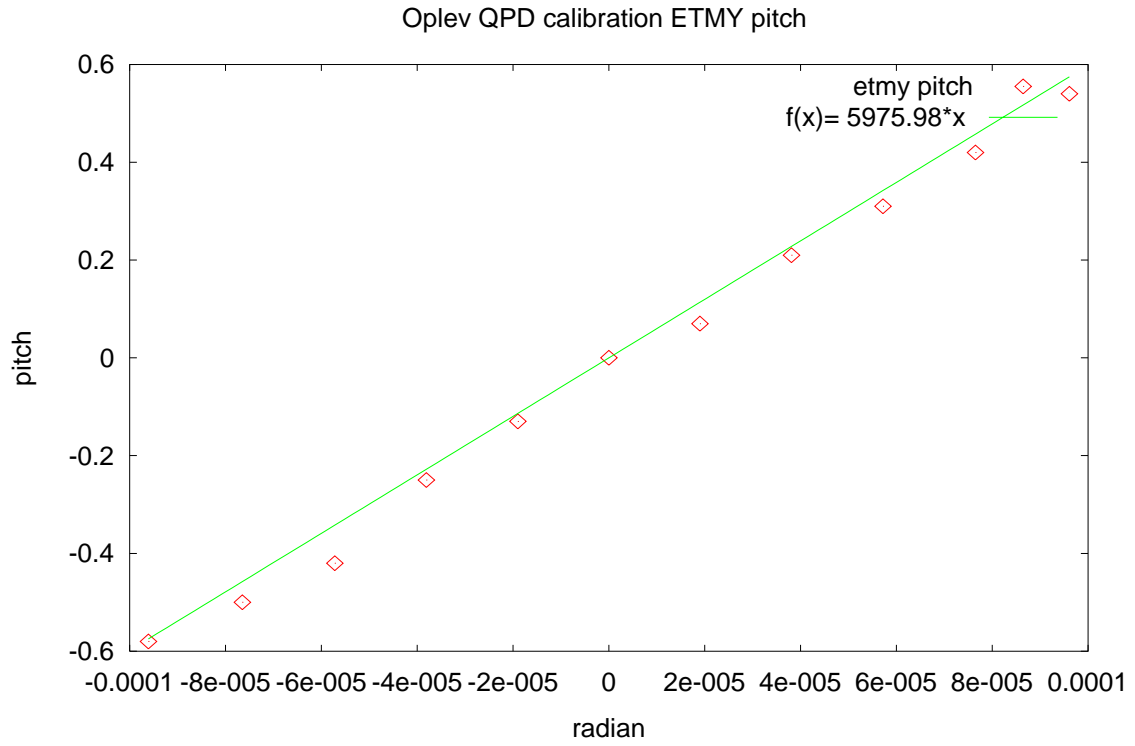


Figure 16: ETMY pitch and yaw

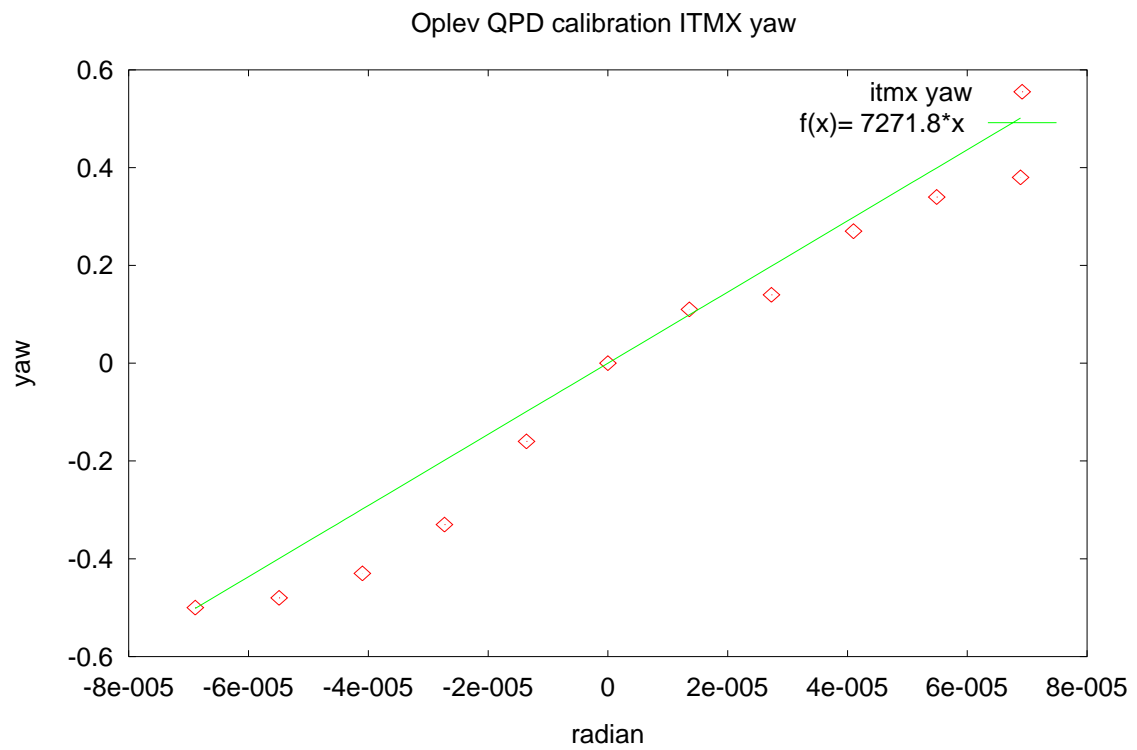
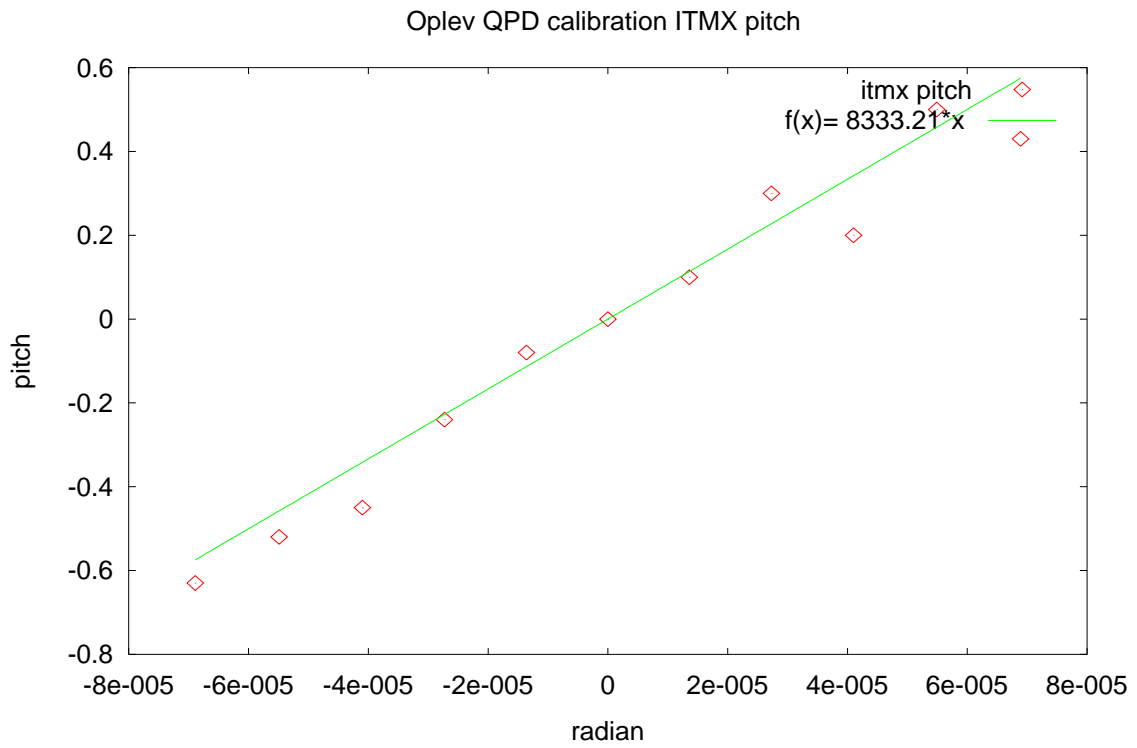


Figure 17: ITMX pitch and yaw

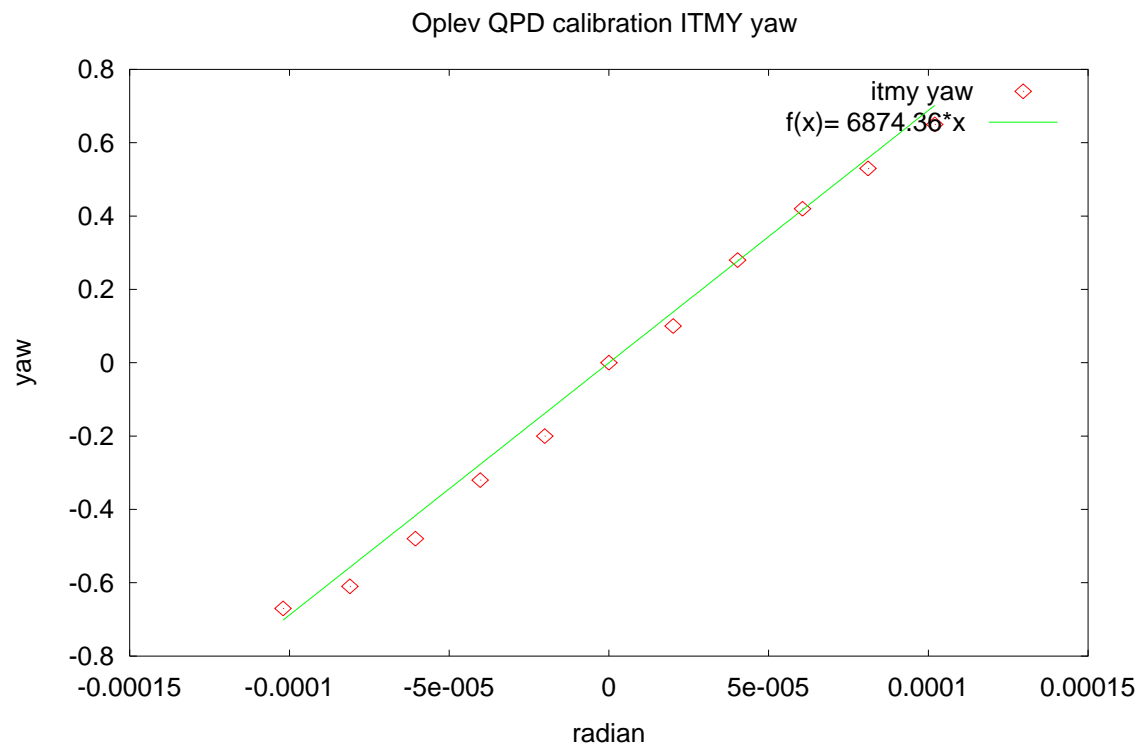
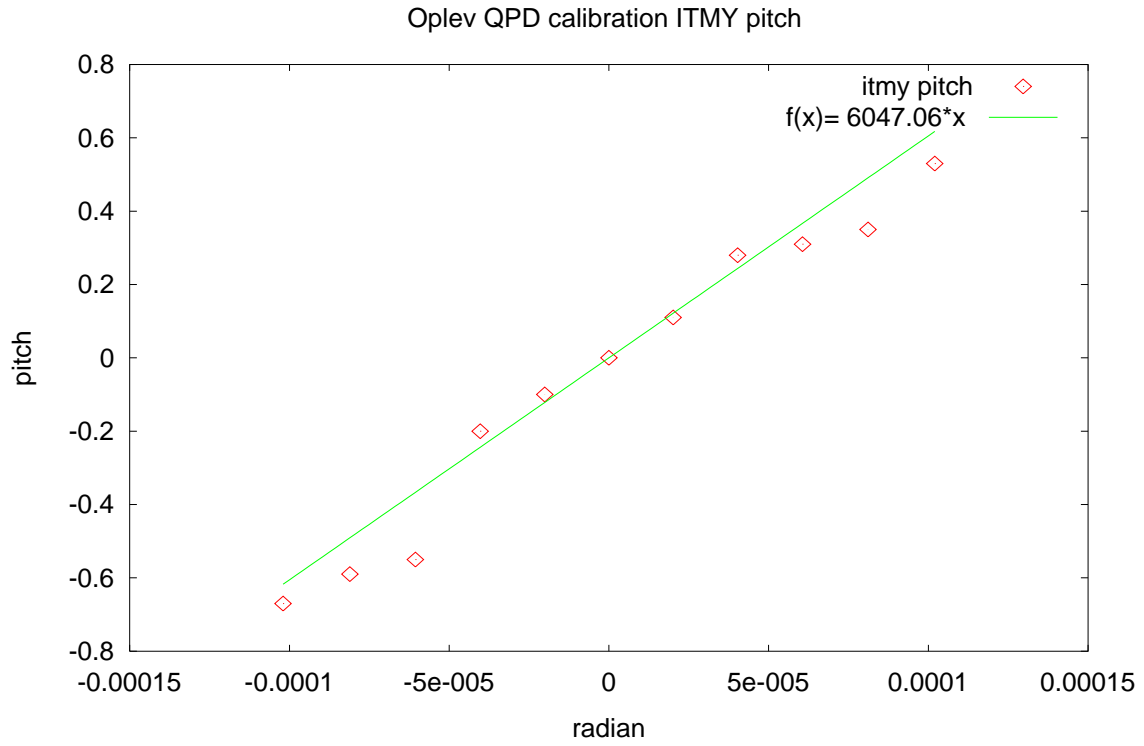


Figure 18: ITMY pitch and yaw

## Appendix 5: The In-loop noise spectra

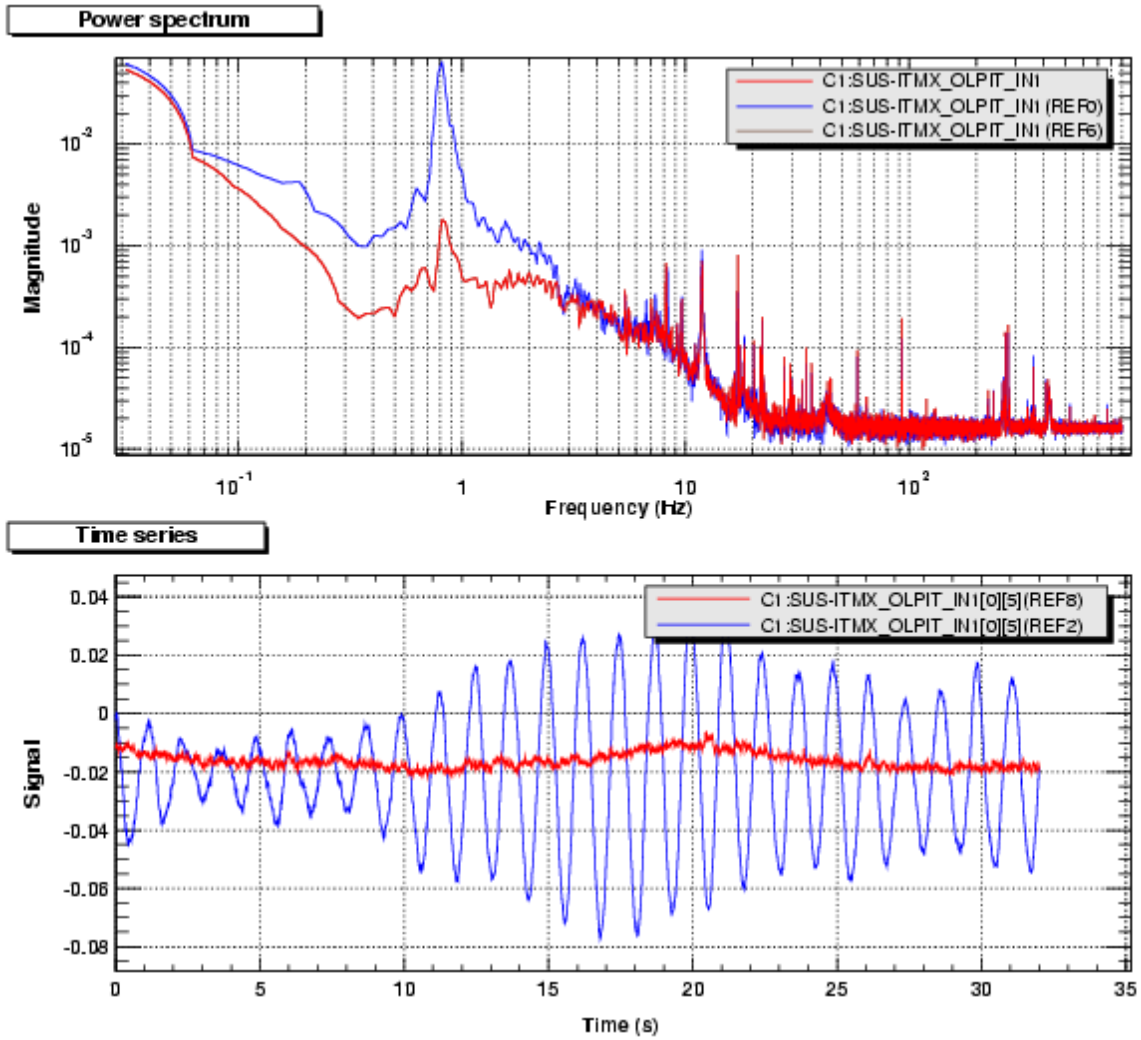


Figure 25: ITMX pitch

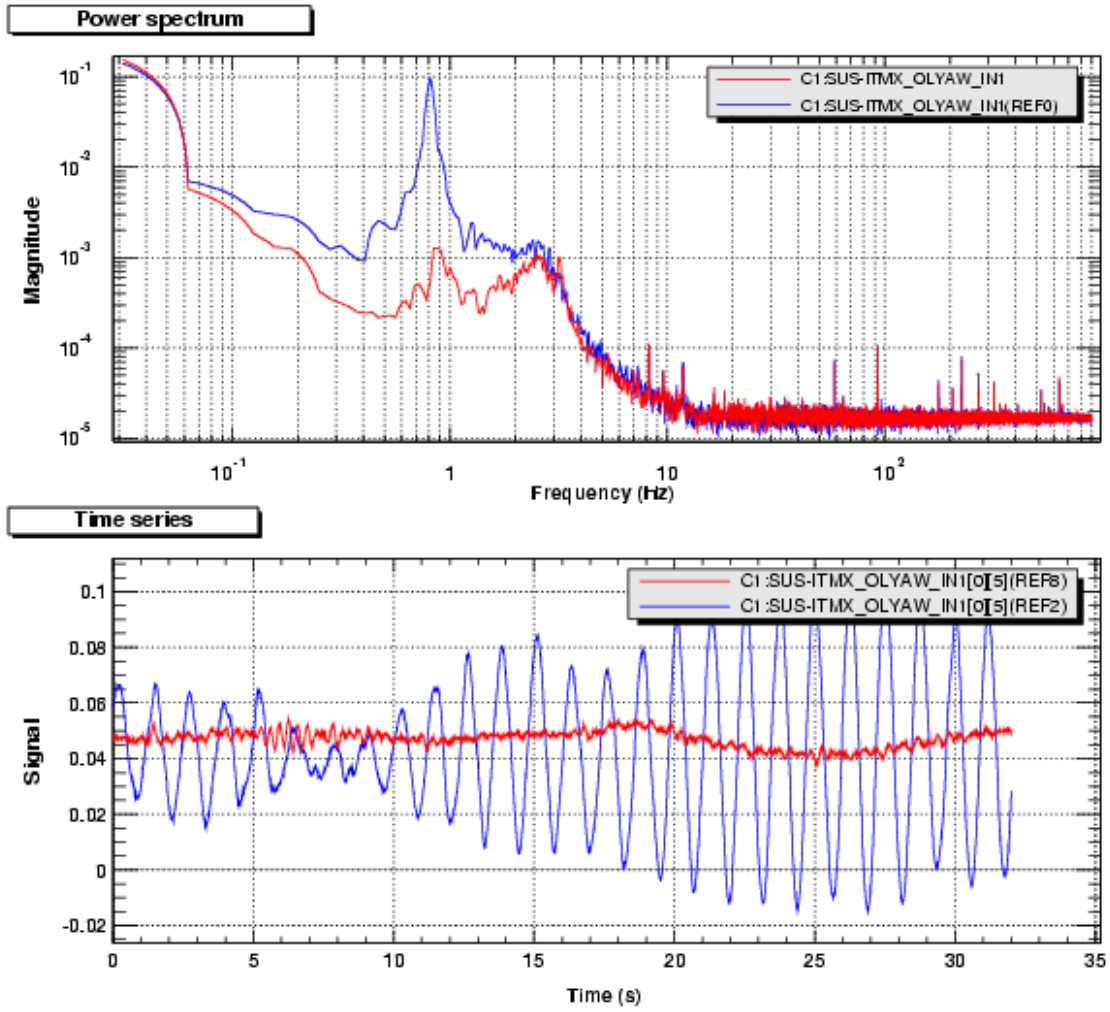


Figure 26: ITMX yaw

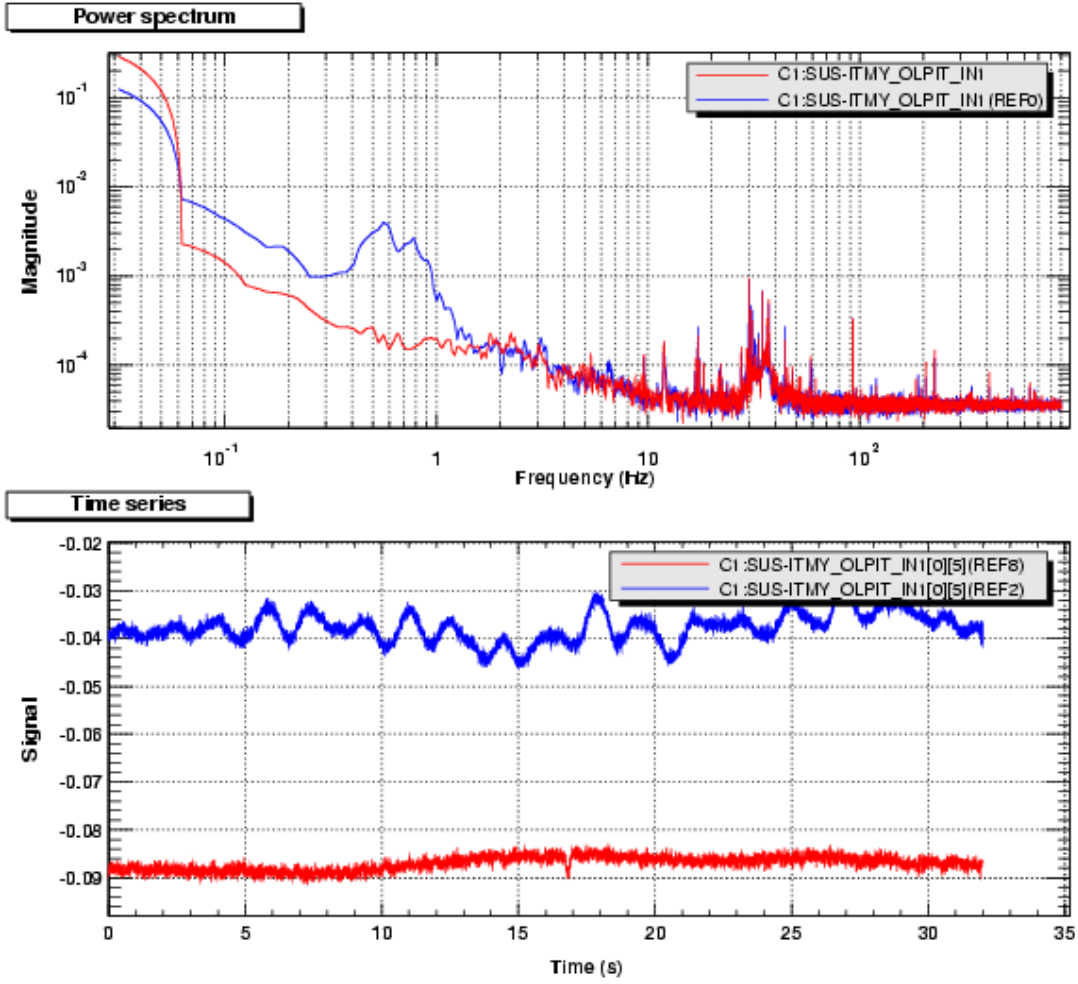


Figure 27: ITMY pitch

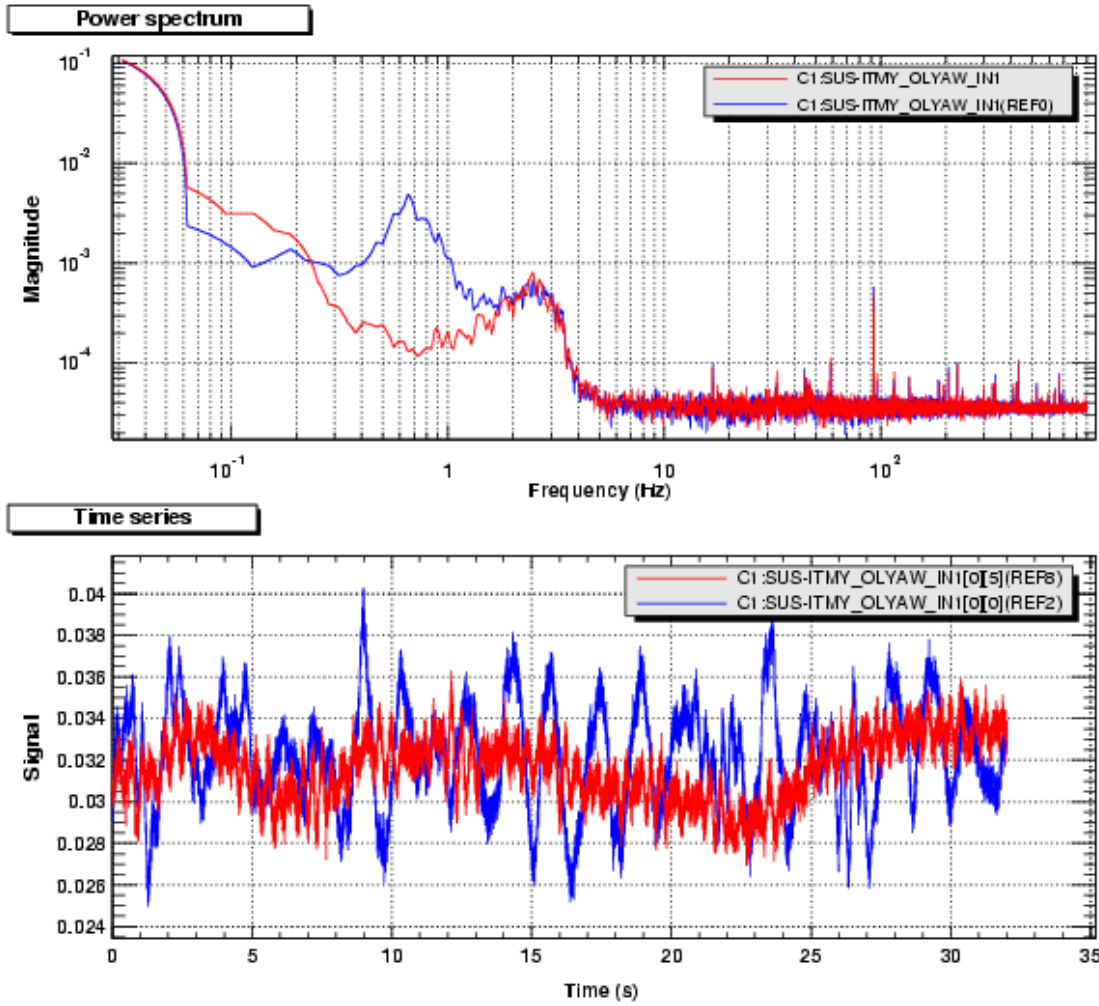


Figure 28: ITMY yaw

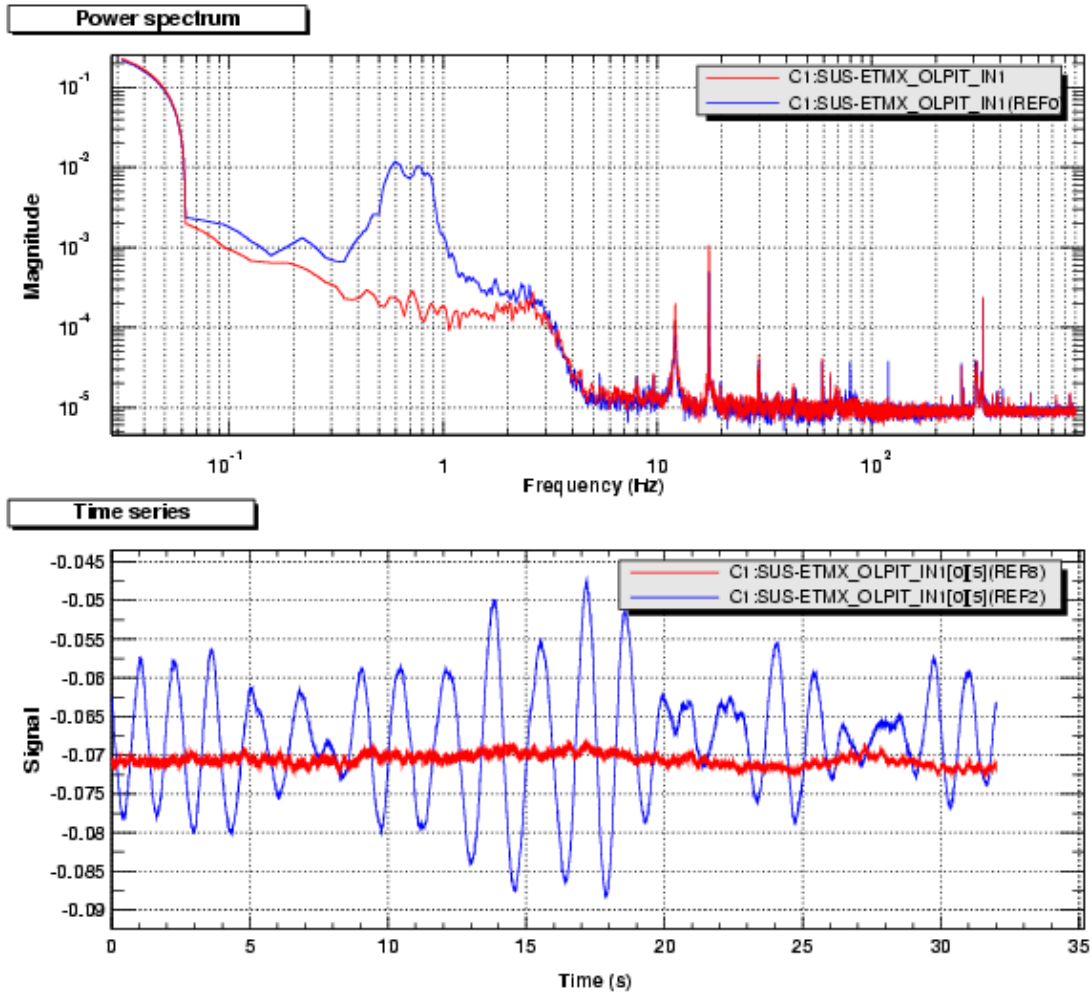


Figure 29: ETMX pitch

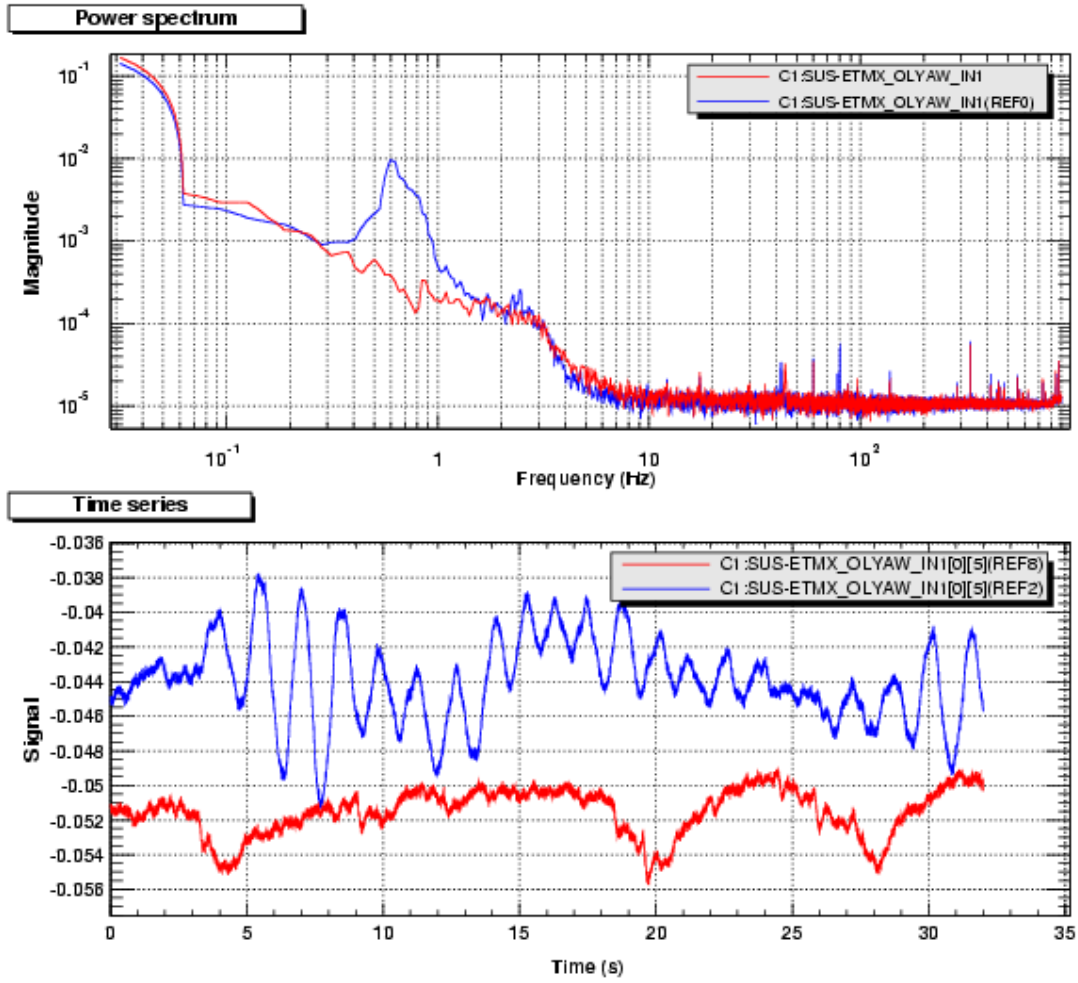


Figure 30: ETMX yaw

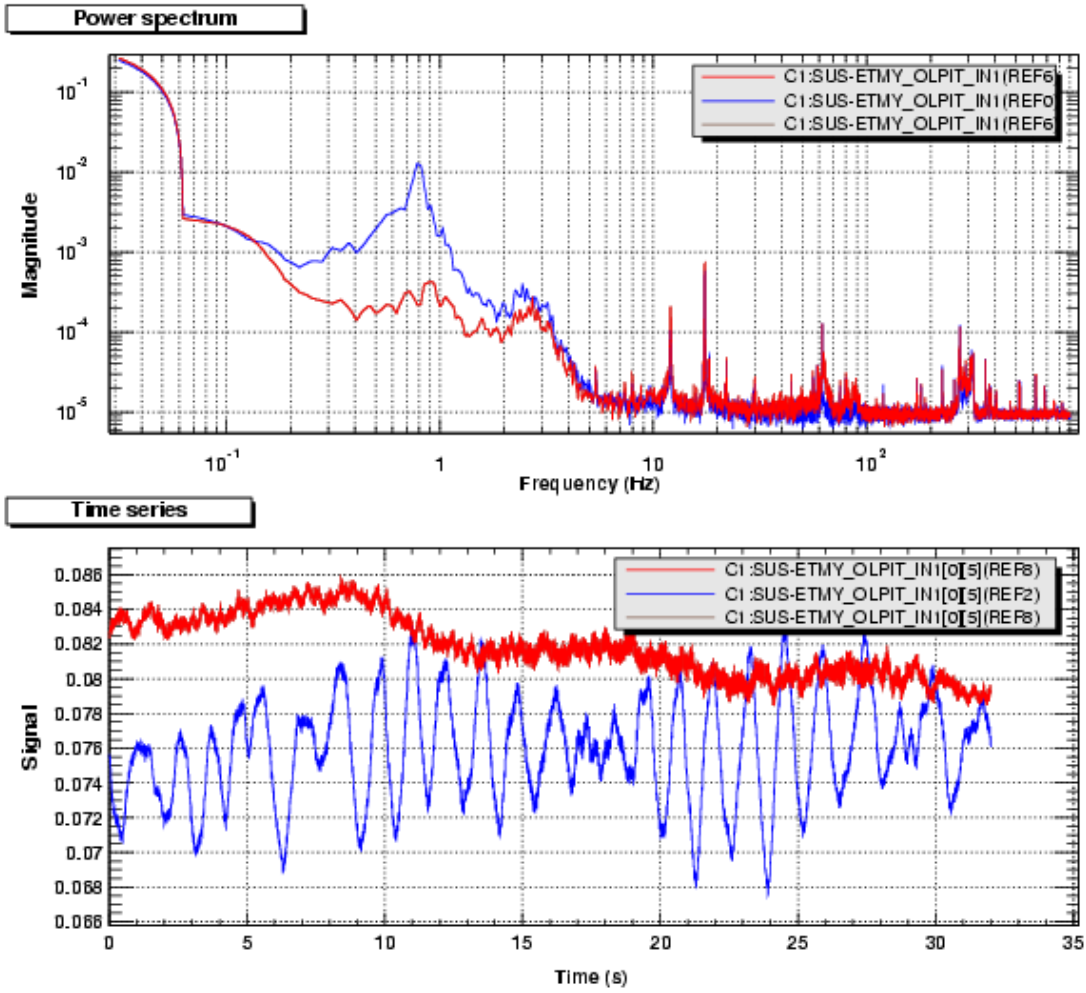


Figure 31: ETMY pitch

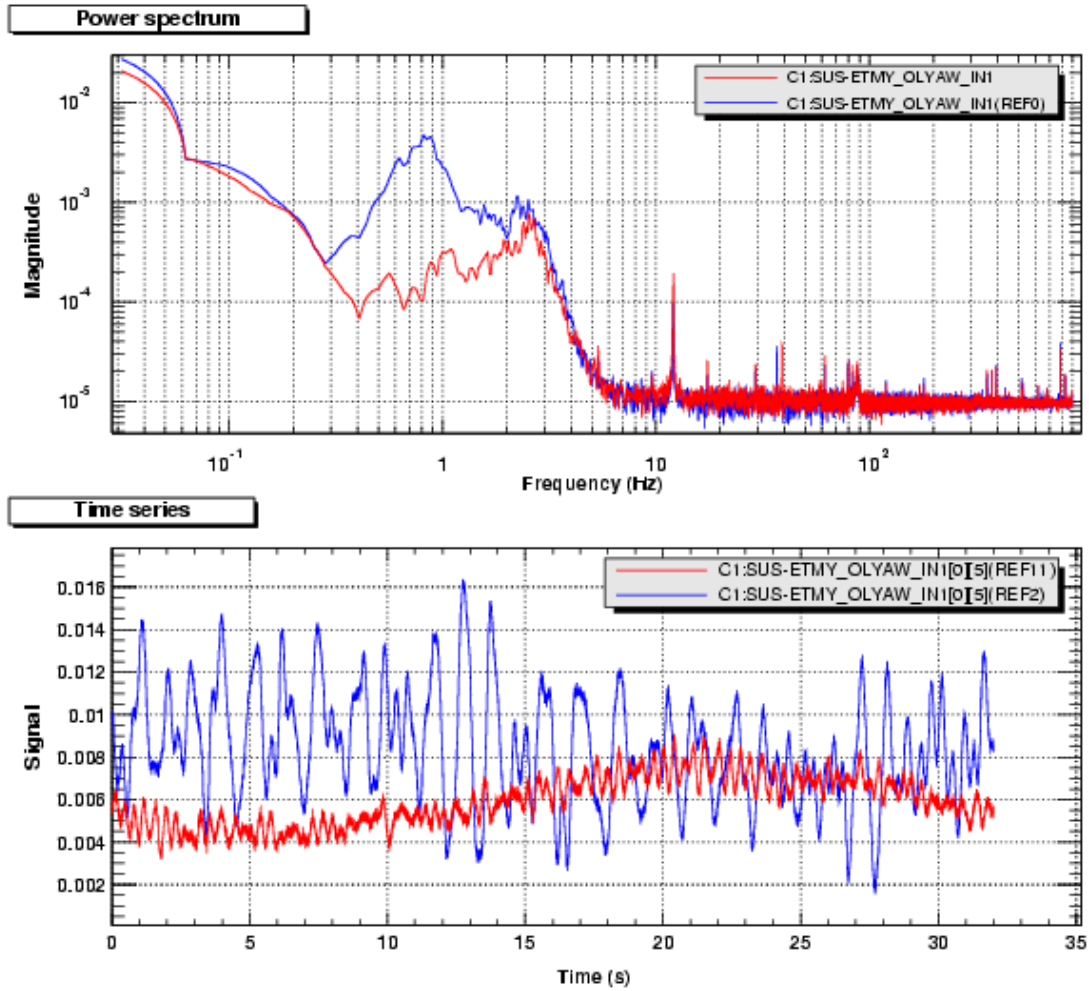


Figure 32: ETMY yaw

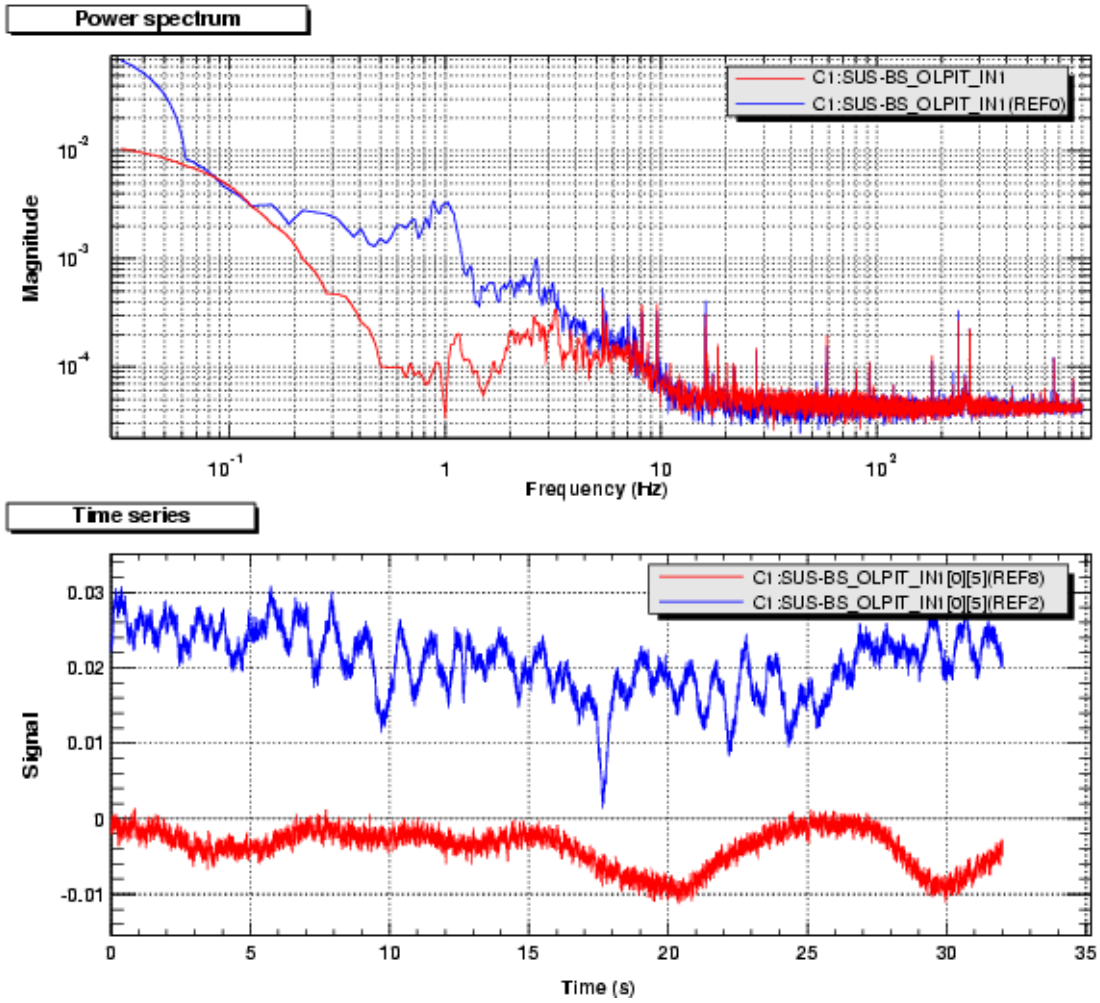


Figure 33: BS pitch

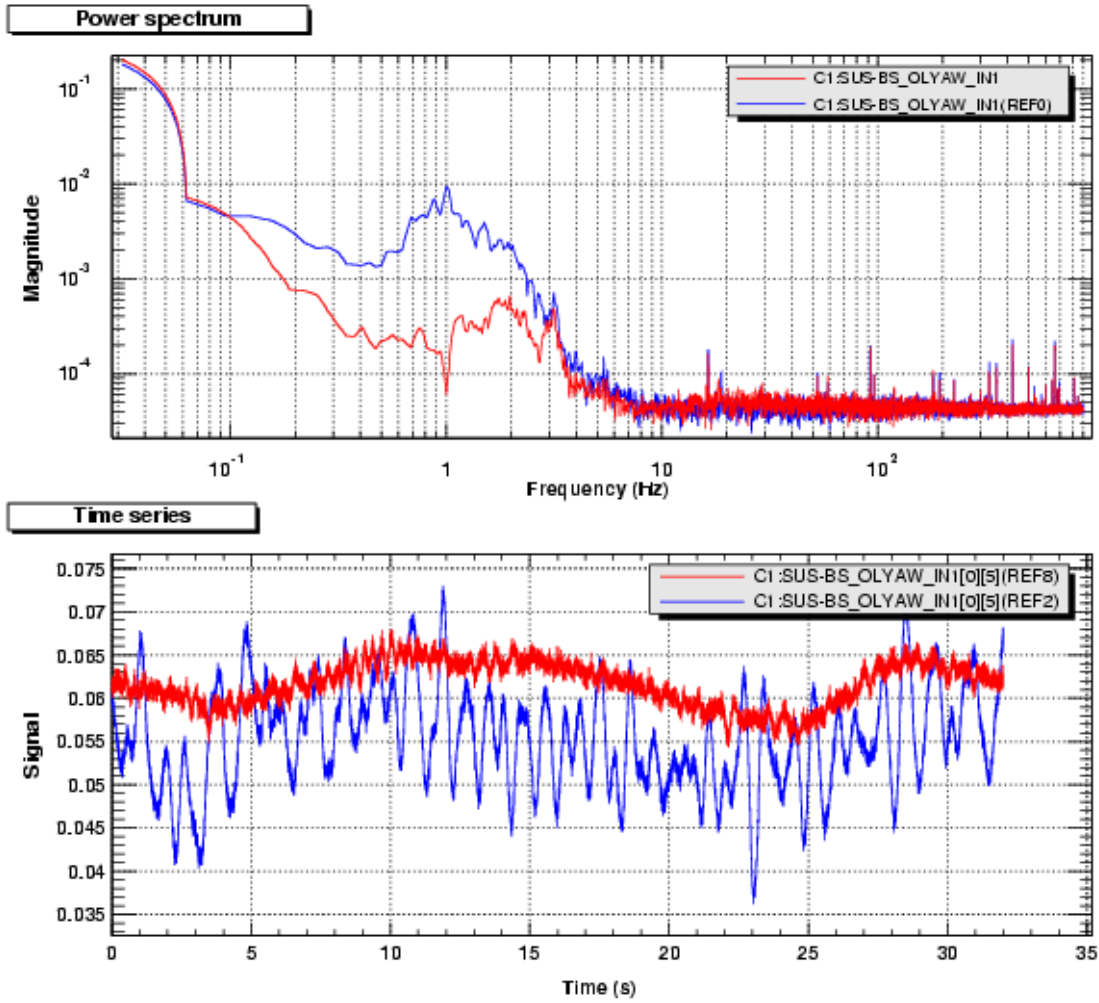


Figure 34: BS pitch

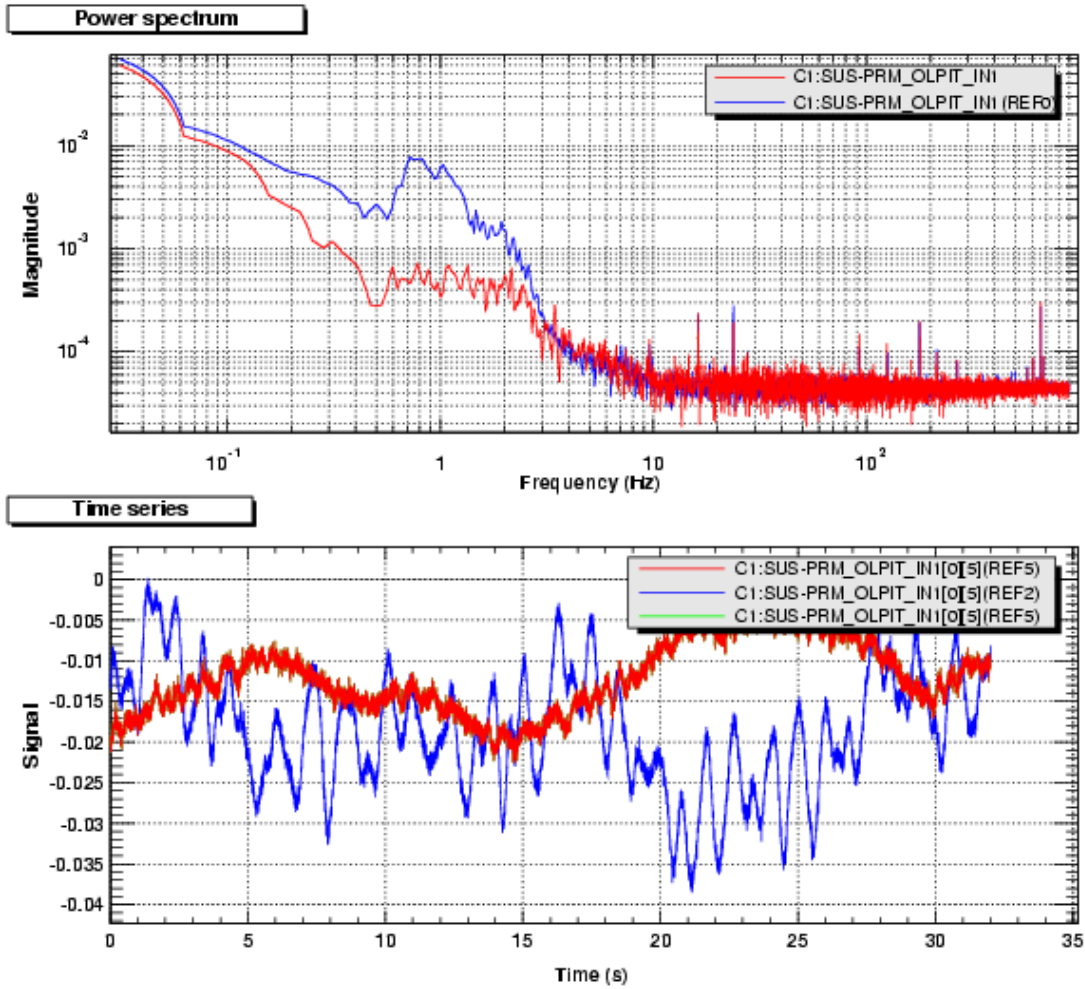


Figure 35: PRM pitch

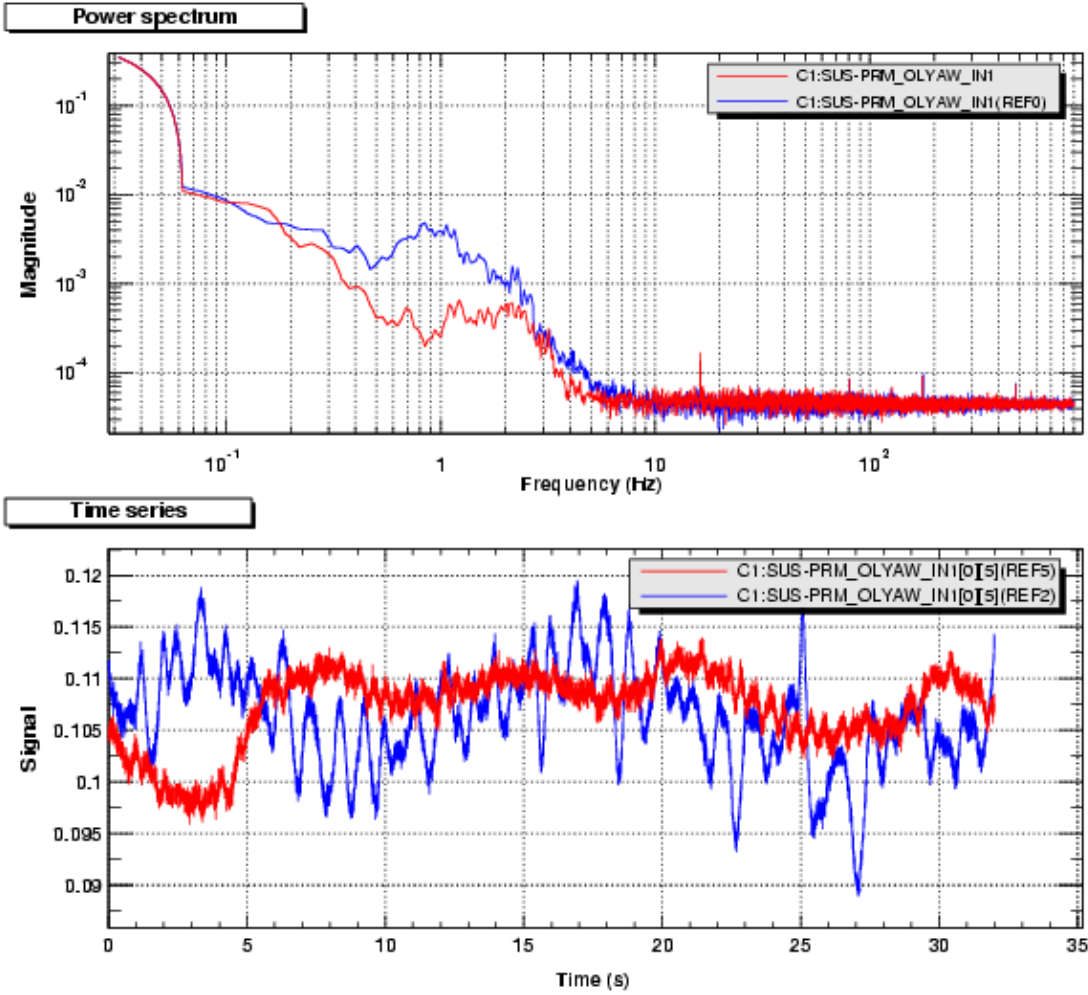


Figure 36: PRM yaw

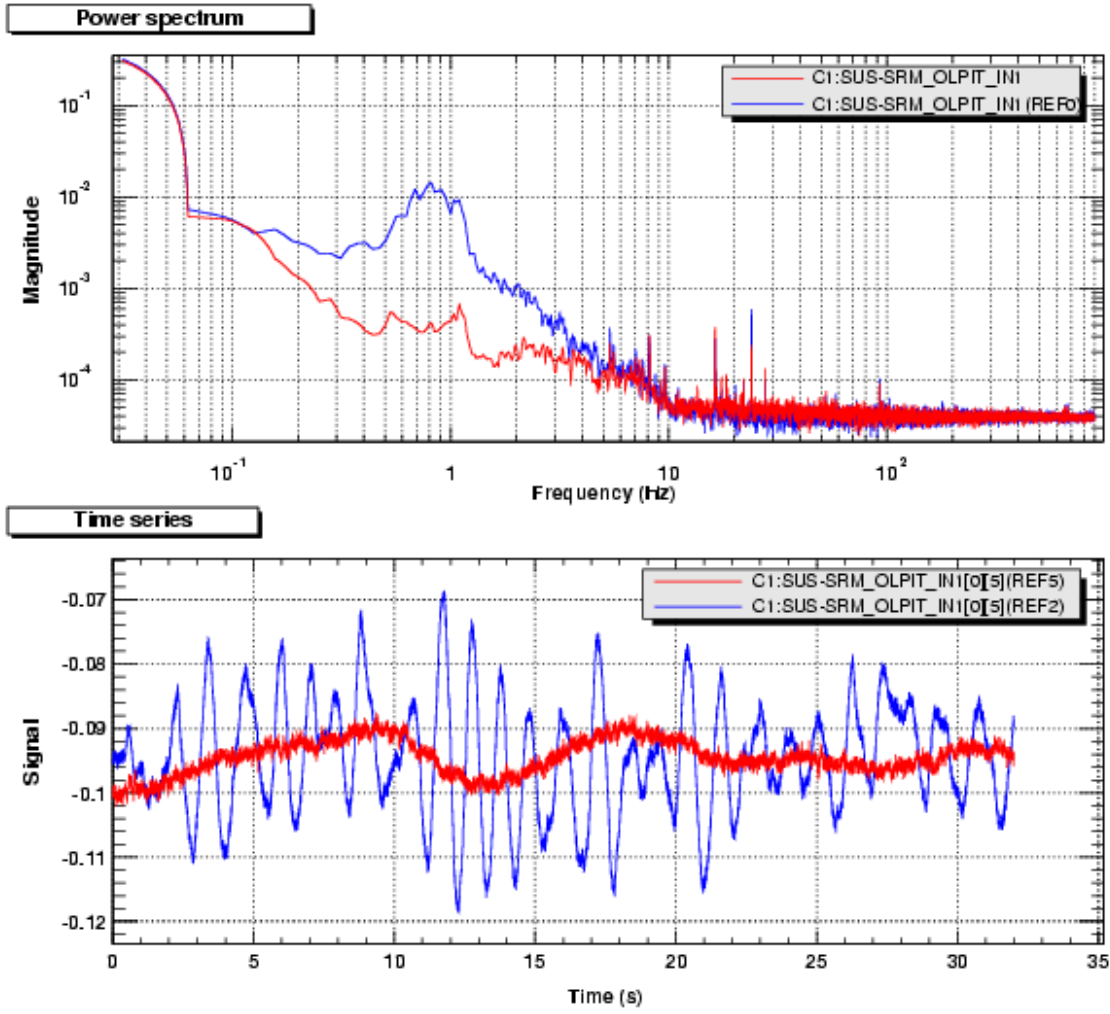


Figure 37: SRM pitch

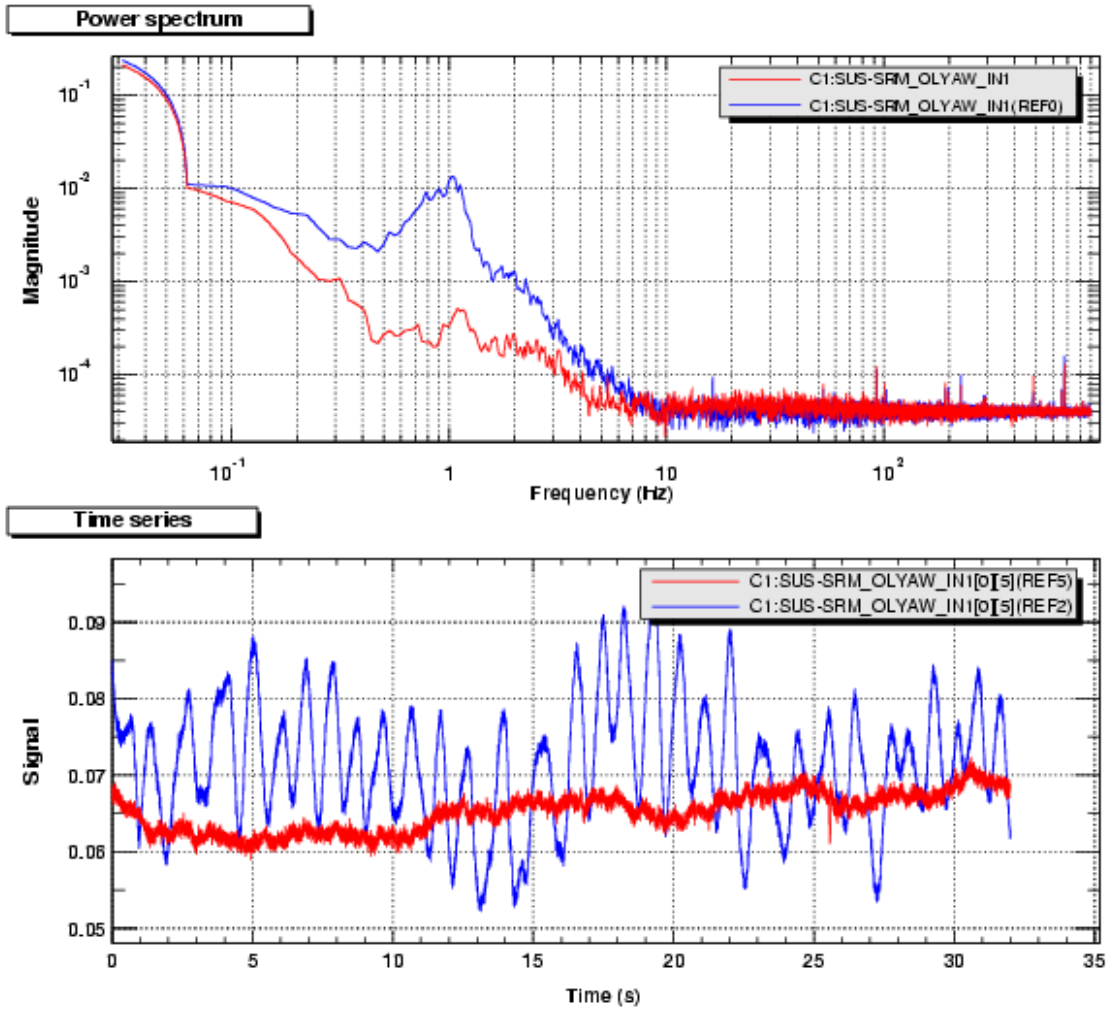


Figure 38: SRM yaw